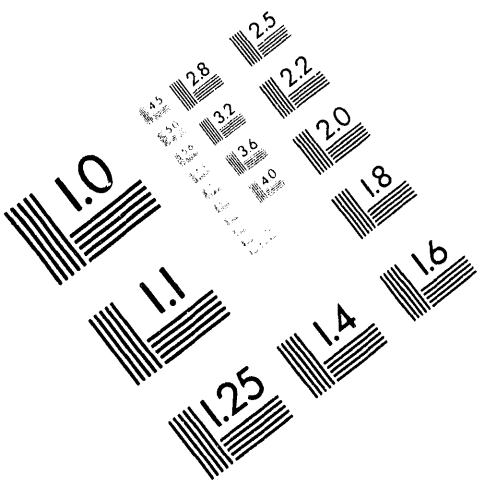

Association for Information and Image Management

1100 Wayne Avenue, Suite 1100
Silver Spring, Maryland 20910

301/587-8202

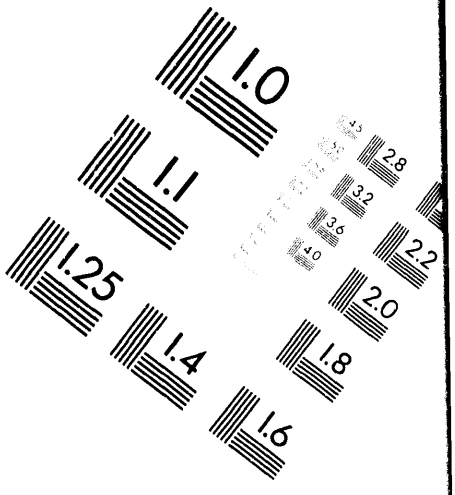

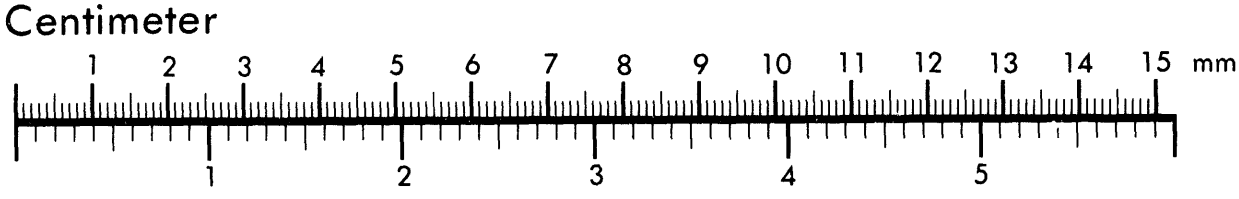

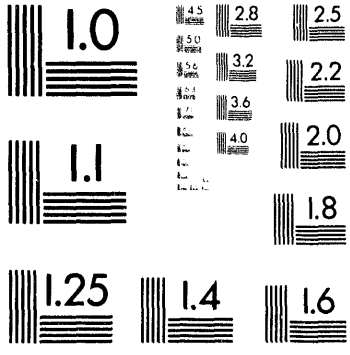

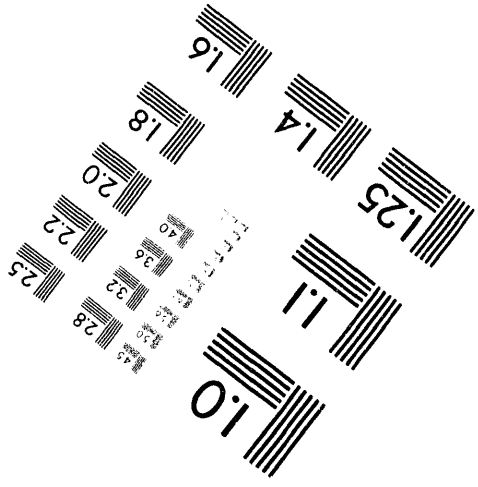

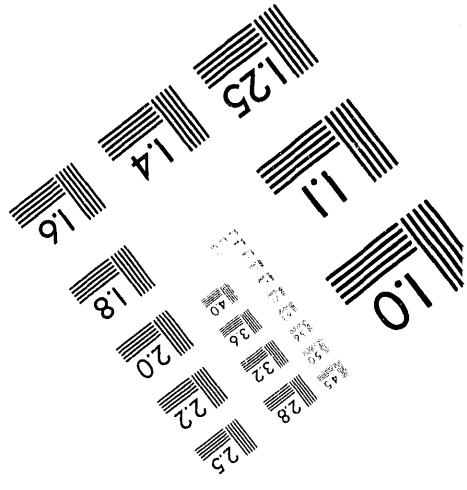

MANUFACTURED TO AIIM STANDARDS
BY APPLIED IMAGE, INC.

1 of 1

40/5-6.94 9S(2)

PREPARED FOR THE U.S. DEPARTMENT OF ENERGY,
UNDER CONTRACT DE-AC02-76-CHO-3073

PPPL-2989
UC-420,421

PPPL-2989

UTILITY OF EXTRACTING α-PARTICLE ENERGY BY WAVES

BY

N.J. FISCH AND M.C. HERRMANN

MAY, 1994

PPPL PRINCETON PLASMA PHYSICS LABORATORY

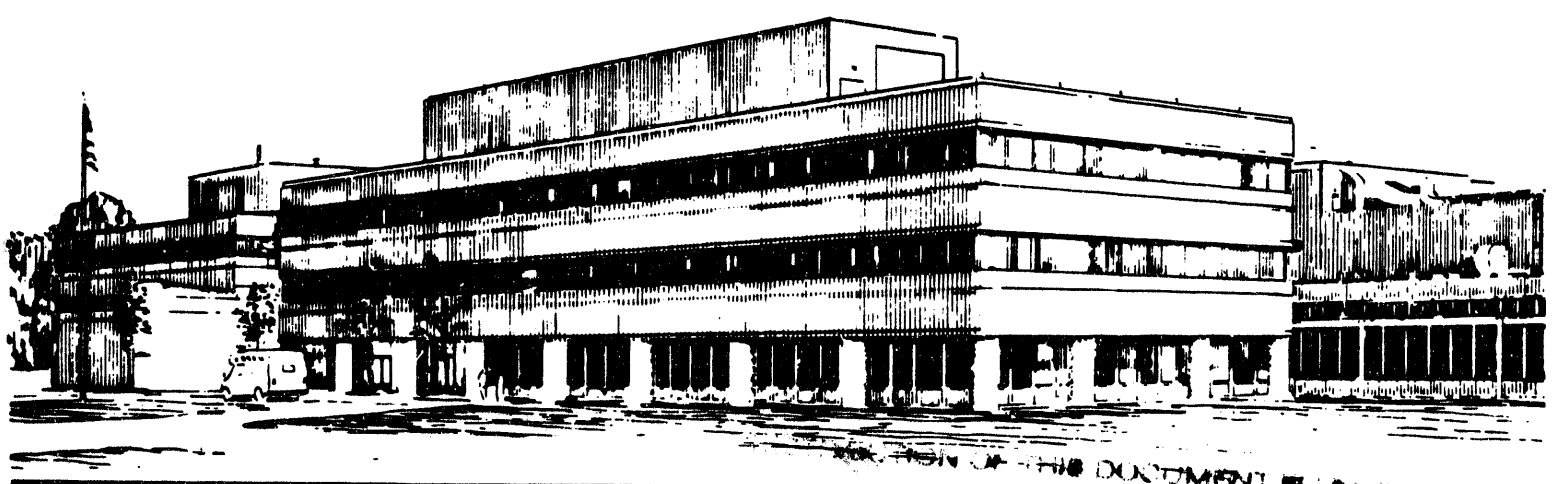

PRINCETON UNIVERSITY, PRINCETON, NEW JERSEY

NOTICE

NOTICE

Utility of Extracting α-particle Energy by Waves

Nathaniel J. Fisch and Mark C. Herrmann

Princeton Plasma Physics Laboratory, P. O. Box 451
Princeton University, Princeton, NJ 08543

The utility of extracting α-particle power, and then diverting this power to fast fuel ions, is investigated. As power is diverted to fast ions and then to ions, a number of effects come into play, as the relative amounts of pressure taken up by electrons, fuel ions, and fast α-particles shift. In addition, if the α-particle power is diverted to fast fuel ions, there is an enhanced fusion reactivity because of the nonthermal component of the ion distribution. Some useful expressions for describing these effects are derived, and it is shown that fusion reactors with power density about twice what otherwise might be obtained can be contemplated, so long as a substantial amount of the α-particle power can be diverted. Interestingly, in this mode of operation, once the electron heat is sufficiently confined, further improvement in confinement is actually not desirable. A similar improvement in fusion power density can be obtained for advanced fuel mixtures such as D-He^3, where the power of both the energetic α-particles and the energetic protons might be diverted advantageously.

1. Introduction

If the energy from energetic α-particles could be extracted by waves and diverted to the tail of the fuel distribution in a tokamak reactor, there are a number of benefits: First, the energetic α-particle pressure is suppressed, allowing for more fuel ion pressure. Second, the electron temperature is suppressed while the ion temperature is enhanced, possibly giving rise to the so-called "hot ion mode". Third, there is a nonthermal fuel ion component that may lead to increased reactivity at a given pressure. On the other hand, there are costs: to divert α-particle power may require external catalytic heating, and, in any event, the increased reactivity leads to more α-particle pressure, which also must be taken into account. What this paper attempts to do is to quantify these benefits and costs.

It has been recognized that there are advantages in attempting to operate fusion reactors in regimes in which there is a significant hot, nonmaxwellian component to the fuel ions,[1-3] or in which the fuel ion temperature can be much greater than the electron temperature.[4,5] Noting a number of experiments[6-8] exhibiting the hot-ion mode, Clarke[5] pointed out that the hot ion mode regime could be reached if the ion energy confinement time exceeds the electron energy confinement time, and that this mode is more easily reached if there would be velocity space instabilities that diverted α-particle power to the fuel ions. Recently, it was recognized that the free energy in the α-particles might be more completely tapped by injecting waves that diffuse the α-particles both in space and energy, rather than just in energy.[9-11] In fact, it appears that, at least in principle, eventually all of the α-particle power could be diverted to the ions.

This paper builds upon the work by Clarke in particular, with the added element that there are now at hand definite ways of tapping the α-particle power by waves, and that, moreover, these waves might then damp resonantly on the fast energy tail of the fuel ions. Thus, not only is the hot ion mode realized through the diversion of α-particle power, as envisioned by Clarke, but a significant nonmaxwellian fusion component is realized simultaneously, as envisioned by Furth, Dawson, and coworkers.

This paper does not address the utility in diverting α-particle power for the purposes of amplifying the current drive effect. The possibilities for significantly less circulating power in accomplishing the current drive effect have been discussed elsewhere.[9] In principle, both enhanced reactivity and enhanced current drive efficiency could be obtained at once if not necessarily optimized at once. Here, our concern will be the benefits of the hot ion mode, and how it might be attained.

It should be noted, however, that what is envisioned as an eventual very much more attractive reactor is considerably different from conventional designs. With substantially all the α-particle power diverted to waves, the envisioned reactor is very much driven by rf waves; there may be several hundred megawatts of rf power flowing through the tokamak. Part of this power is injected (perhaps up to 100–200 MW), and the remainder arises from amplification by the α-particles (perhaps up to 400–800 MW). The rf waves increase the fusion power density, accomplish current drive, and tend to expel the α-particles in the process of extracting energy, thus accomplishing ash removal. In addition, confinement times tend to be short, especially the electron heat confinement time. Both of these aspects tend to push the plasma far from thermal equilibrium, allowing both for ion temperatures that are far in excess of electron temperatures and for nonthermal features in the ion

velocity distribution.

The paper is organized as follows: In Sec. 2, the effect of diverting a small amount of power at constant β is examined. This incremental posing of the problem is useful, among other reasons, for isolating and understanding the different effects that come into play upon diverting power. In Secs. 3, 4, and 5, these various effects are quantified and discussed. In Sec. 6, a global approach is taken to find operating points that give self-consistent burn. In Secs. 7 and 8, analytic expressions are given for ignition or self-consistent burn in the hot ion mode. Some useful limiting cases are examined in which progress can be made analytically. In Sec. 9, a number of examples of self-consistent burn parameters are calculated numerically. These examples illustrate the advantages of diverting α-particle power in a variety of settings. In Sec. 10, contour plots are introduced that depict how optimized operating points can be found. These plots are very useful in navigating through parameter space to reach optimum reactor performance, whether defined by doubling the fusion power density, or by optimizing in some other way, such as by reducing the necessary heat confinement times. The point is made in Sec. 11 that similar increases in fusion power density are available through diverting the charged fusion products in a D-He^3 reactor. A summary of our findings is presented in Sec. 12.

2. Incremental Diversion of α-particle Power

In quantifying the benefits and costs of diverting α-particle power to fast fuel ions, it is necessary to clarify how this problem can be posed. One way of posing this problem is to begin with a reactor design, presumably designed to operate at ignition and at maximally allowable pressure, and to ask what would be the net effect of diverting some small amount of α-particle power Δp, that normally would have gone to electron heating and now is to go to superthermal fuel ion heating. (Note that the quantity Δp is not quite the diverted power, since some of the diverted power might in any event have been absorbed by ions, and that part would not count in Δp.) This is the so called "incremental" posing of the problem.

This posing of the problem should quantify the utility of an auxiliary system to an operable reactor, where that auxiliary system extracts extra fusion power from the reactor without changing its operating design, particularly with respect to maintaining the total plasma pressure. There are, however, a number of subtleties here. How exactly is the plasma pressure to be maintained, if extra fusion power, together with the associated extra plasma heating, is the result of diverting this small amount of power? This is intimately related to the question of burn control, which in any event must be a part of the reactor design.

In order to pose the incremental problem sensibly, without going into the details of a specific reactor design, let us assume that burn control is essentially exercised by the prompt loss of some α-particles. These α-particles then do not contribute to the plasma heating, nor do they contribute to the plasma pressure, nor is the power here available for diversion to the ions. By adjusting the rate of these prompt losses, plasma equilibrium at constant plasma pressure can be maintained.

Thus, in quantifying the effect of enhanced reactivity, we shall not consider, in the incremental problem, the effect of the enhanced reactivity on the plasma operating regime; specifically, we shall assume that any extra fusion power produced is somehow promptly

lost so that it neither further heats the plasma nor contributes to the energetic α-particle pressure, with the provision that in order to maintain the plasma at constant pressure, the precise amount of α-particle power available to indeed heat the plasma and to contribute to the plasma pressure may be adjusted through the burn control. In this regard, i.e., to remain at constant pressure, we imagine too that upon diverting power it may even be necessary to adjust the base level (excluding the enhanced production) of α-particle power that is deposited within the plasma.

This posing of the incremental problem is not unique. For example, an alternative posing of the problem might be to imagine a subignited plasma, with flexibility maintained over the external heat source. A second example might be to allow for an adjustment in the energy confinement times of the fuel ions and electrons. Indeed, with the flexibility to tamper individually with these confinement times, somewhat more optimistic results could be obtained. The present posing, however, appears to be both pristine and simple, while capturing the essential physics. The key question to be answered here is how many extra fusion watts can be captured for every watt of α-particle power that is diverted. An add-on system will be economical if this number is large, assuming the cost to divert power is small.

While the incremental problem addresses the question of net power amplification, in practice, if there is power multiplication, one is interested in how much extra fusion power is in fact available. Here, an important limitation in a D-T reactor is that only 20% of the fusion energy released is in the form of α-particles and so may be exploited. On the other hand, if by diverting α-particle power, more α-particle power is produced, this further power might also be diverted to advantage. This leads to a "maximal" rather than "incremental" posing of the problem—exactly how big of an effect is possible. Suppose that all the α-particle power could be diverted, and there is the possibility of using external heating; can a reactor be made significantly better?

In the next three sections, we pose the incremental problem and we show that quite large energy multiplications are in principle obtainable. These sections are useful for understanding in detail the competing effects that occur upon diverting power. In the remainder of the paper, we consider a maximal or global posing of the problem, which is of more immediate consequence. Here, we find reactor regimes in which the fusion power density is increased by about a factor of two.

3. Enhanced Ion pressure from Diverting Alpha Particle Power

Suppose that a quantity of α-particle power Δp is diverted from electron heating to ion heating. To calculate the increase in reactivity, we use a 0-D model of the heat flow,

$$\frac{d}{dt}\beta_e = \nu(\zeta\beta_i - \beta_e) + p_e - \beta_e/\tau_e \tag{1}$$

$$\frac{d}{dt}\beta_i = \nu(\beta_e - \zeta\beta_i) + p_i - \beta_i/\tau_i, \tag{2}$$

where $\beta_e = 3n_eT_e/2$ is the electron pressure, β_i is the ion pressure, ν is the temperature equilibration rate, τ_e and τ_i are the electron and ion energy confinement times, and p_e and p_i are the external heating power to electrons and ions, including α-particle power. Here,

we defined $\zeta \equiv \sum_j n_j Z_j / \sum_j n_j$, which is the ratio of electron to ion densities, with Z_j defined as the ion charge state for the jth species. Suppose for simplicity a pure hydrogen plasma, so that $\zeta = 1$. To find the steady state operating pressures, solve Eqs.(1) and (2) with $d/dt = 0$ to obtain

$$\beta_i = \frac{p_e + (1 + 1/\nu\tau_e)p_i}{D} \tag{3}$$

$$\beta_e = \frac{p_i + (1 + 1/\nu\tau_i)p_e}{D}, \tag{4}$$

where

$$D = \frac{1}{\tau_i} + \frac{1}{\tau_e} + \frac{1}{\nu\tau_e\tau_i}. \tag{5}$$

Now what happens if a quantity of α-particle power Δp is diverted from electron heating to ion heating? Absent any other effects, it may be seen from Eqs.(3) and (4) that the total plasma pressure is not necessarily constant. After all, there is no reason, a priori, to expect that the plasma is equally able to contain electron heat and ion heat. The plasma, however, must operate below a maximum total pressure, and, if the plasma parameters are chosen optimally, we may assume that the operation is in fact at the maximum pressure for any Δp. As discussed in Sec. 2, if power is diverted at constant pressure, one must also change incrementally either the confinement times or the total power input. It might be reasonable to expect that control is more easily exercised over the power input, for example, by designing the operating point at somewhat different α-particle heating. Thus, choose the alpha particle heating so as to remain at the maximum pressure by supposing that

$$p_i = (1 - \theta)p_{i0} + \Delta p, \tag{6}$$

$$p_e = (1 - \theta)p_{e0} - \Delta p, \tag{7}$$

where θ is the incremental fractional change in alpha heating for finite Δp that assures that operation is at constant total pressure, i.e.,

$$\beta \equiv \beta_e + \beta_i = \beta_{e0} + \beta_{i0}. \tag{8}$$

Substituting Eqs.(6) and (7) into Eqs.(3) and (4) and using Eq.(8), results in three linear equations in the three unknowns β_i, β_e and θ, with solutions such that the plasma achieves a new equilibrium at

$$\theta = \frac{\Delta p}{\nu D}\left(\frac{1/\tau_e - 1/\tau_i}{\beta_{e0} + \beta_{i0}}\right). \tag{9}$$

where β_{e0} and β_{i0} are the equilibrium pressures in the absence of any power diversion. Note that for $\tau_i > \tau_e$, then $\theta > 0$, indicating that less α-particle power maintains the plasma at the maximum pressure. If we write

$$\beta_i = \beta_{i0} + \Delta\beta_i$$

$$\beta_e = \beta_{e0} + \Delta\beta_e,$$

then we have $\Delta\beta_i = -\Delta\beta_e \equiv \Delta\beta$ with

$$\Delta\beta = \frac{\Delta p}{\nu D}\left(\frac{\beta_{e0}/\tau_e + \beta_{i0}/\tau_i}{\beta_{e0}+\beta_{i0}}\right). \tag{10}$$

The ratio $\Delta\beta/\Delta p$ can be thought of as the incremental efficiency in diverting power to increase β_i.

Note that constant plasma pressure is maintained by adjusting the α-particle heating power $P_\alpha \to (1-\theta)P_\alpha$. Although this keeps the sum of the fuel ion and electron pressure constant, the change in the number of energetic α-particles present to maintain the plasma pressure does affect the α-particle pressure as addressed in Sec. 4.

4. Enhanced Ion Pressure from Reducing α-Particle Pressure

Suppose that most of the α-particle pressure is taken up by the fast nonmaxwellian component. One can then write $\beta_{\alpha H} = P_\alpha \tau_\alpha$, where P_α is the α-particle power and τ_α is the α-particle slowing down time. Now if Δp is diverted from the α-particles into fast ions, the change in the the α-particle pressure is $\Delta\beta_{\alpha H} = -\Delta p \tau_\alpha$.

When the α-particle power is diverted into fast fuel ions, the fast fuel ions at say 100 keV slow down quickly compared to the 3.5 MeV α-particles. In the maximal posing of the problem as addressed in later sections, the energetic fuel ion pressure is taken into account. For simplicity here, however, we neglect the fast ion pressure (see Appendix A). The extra pressure available to the plasma, which must be shared between electrons and ions, is then just the amount lost by the α-particles. Thus, if the total fixed plasma pressure is $\beta_0 \equiv \beta_e + \beta_i + \beta_{\alpha H} = \beta_i(1+\beta_e/\beta_i) + \beta_{\alpha H}$, then for a fixed ratio $\beta_e/\beta_i = \beta_{e0}/\beta_{i0}$, one recovers the change in β_i due to the decreased α-particle beta upon diverting power Δp as

$$\Delta\beta_i^{(1)} = -\frac{\Delta\beta_{\alpha H}}{1+\beta_e/\beta_i} = \frac{\Delta p \tau_\alpha}{1+\beta_{e0}/\beta_{i0}}. \tag{11a}$$

The enhanced fusion reactivity leads to more α-particles and hence more fast α-particle pressure, but the number of α-particles retained, in the incremental model, are only sufficient to maintain the total plasma pressure. The α-particle power available to heat the plasma is, from Eqs. (6) and (7), changed by an amount $\Delta P_\alpha = \theta P_\alpha$. Thus, in addition to the decrement in $\beta_{\alpha H}$ upon diverting power Δp, there may be an an additional difference, if $\theta \neq 0$. This results from the altered operating regime, since less or more α-particle power need be absorbed to maintain the plasma pressure, this difference being $\Delta P_\alpha = -\theta P_\alpha$. Using Eq.(9), the increase in the available fuel ion pressure is then

$$\Delta\beta_i^{(2)} = \frac{\theta P_\alpha \tau_\alpha}{1+\beta_{e0}/\beta_{i0}} = \frac{\Delta p}{\nu D}\left(\frac{1/\tau_e - 1/\tau_i}{\beta_{e0}+\beta_{i0}}\right)\frac{P_\alpha \tau_\alpha}{1+\beta_{e0}/\beta_{i0}}, \tag{11b}$$

which is in addition to the term in Eq.(11a).

5. Incremental Enhanced Fusion Production

Recall that there are two contributions to the enhanced fusion production in diverting α-particle power: one is from the production of fast nonthermal ions and the other is

from an increase in the thermal ion pressure which arises because thermal ions are directly heated and because the α-particle pressure is reduced.

The production of fusion α-particles from the former effect is directly proportional to the amount of power diverted. As discussed above, for simplicity of presentation, we shall neglect in the incremental posing the pressure of these fast ions. The enhanced fusion production can be written as $\Delta p \chi_\alpha$, where χ_α can be treated, for simplicity here, as a constant (see Appendix A).

The production of fusion α-particles from the latter effect can be written, assuming ion temperatures that optimize the fusion power at constant pressure, as

$$P_\alpha \sim c\beta_i^2, \tag{12}$$

where c is a constant. Thus, the incremental power produced upon realizing an incremental increase in ion pressure is

$$\frac{\Delta P_\alpha}{P_\alpha} \simeq 2\frac{\Delta\beta_i}{\beta_i}. \tag{13}$$

Consider now the increase fusion power resulting from an increase in the thermal ion pressure. Suppose that the only heating is from α-particles with

$$p_e = (1-\eta)P_\alpha$$

$$p_i = \eta P_\alpha,$$

so that from Eq.(3) we have

$$\frac{P_\alpha}{\beta_i} = \frac{D}{1+\eta/\nu\tau_e}. \tag{14}$$

Using now Eqs. (10) and (11) for $\Delta\beta_i$, we get from Eq.(13)

$$\Delta P_\alpha \simeq \Delta p\Bigg\{\chi_\alpha + \frac{2}{\nu+\eta/\tau_e}\left(\frac{\beta_{e0}/\tau_e+\beta_{i0}/\tau_i}{\beta_{e0}+\beta_{i0}}\right) + \left(\frac{2D}{1+\eta/\nu\tau_e}\right)\left(\frac{\tau_\alpha}{1+\beta_e/\beta_i}\right)\left[1+\frac{P_\alpha}{\nu D}\left(\frac{1/\tau_e-1/\tau_i}{\beta_{e0}+\beta_{i0}}\right)\right]\Bigg\}, \tag{15}$$

where the first term on the right is the incremental fast ion fusion, the second term is the enhanced β_i due to the diversion of power from electrons to ions, and the third term is comprised of two parts due to the availability of extra fuel pressure because of the decrease in fast ion pressure, the first part arising from the direct diverting of fast α-particle power and the second part arising from the decreased amount of α-particle heating needed to maintain the plasma pressure upon diverting α-particle power should τ_i be greater than τ_e.

To assess the power multiplication available upon an incremental power diversion, consider a D-T reactor operating such that $\tau_e \simeq \tau_i \equiv \tau$ and such that $\nu\tau \gg 1$. Then Eq.(15) simplifies somewhat to

$$\Delta P_\alpha \simeq \Delta p\left[\chi_\alpha + \frac{2}{\nu\tau} + 2\frac{\tau_\alpha}{\tau}\right]. \tag{16}$$

It is interesting to note that for better confinement times, the incremental advantage in diverting power is less. This is because, for good confinement, it is relatively more difficult to achieve the nonmaxwellian features that enhance the reactivity. On the other hand, poor confinement now has certain advantages.

For a 50:50 DT mixture, one can expect $\chi_\alpha \simeq 1/4$. For the ARIES-I parameter regime, one has $\tau_\alpha/\tau \simeq 1/6$ and $\nu\tau \simeq 3$. Thus, one can expect about 1/4+2/3+1/3=5/4 α-particle watts back for every α-particle watt diverted in such a reactor. Considering that there are about 6.4 total fusion watts, including blanket reactions, for each α-particle watt produced, one has an energy multiplication of 8 watts of fusion for each diverted watt.

What remains to be calculated is how many watts of external power it takes to divert a watt of α-particle power. In principle, the α-particle free energy could be tapped without any external source of power, but that is very unlikely to happen. Suppose, for example, it takes M watts to divert one watt, with the heating power amplified by the diverted watt as it heats the energetic fuel ions. Suppose further that there are enhanced losses of electron power to accomodate the increase in ion heating so that the reactor operating regime remains at constant pressure. Then the heating power watt itself contributes to both enhanced fast ion reactivity as well as to enhanced ion temperature relative to electron temperature. Any extra α-particle power produced, in the incremental posing of the problem, is assumed lost. Thus, in the limit in which Eq.(16) is valid, the extra production of α-particle power due to heating power $p_H = M\Delta p$ is

$$\Delta P_\alpha \simeq p_H \left(\chi_\alpha + \frac{2}{\nu\tau}\right). \tag{17}$$

Suppose a ratio of fusion to α-particle power of $\epsilon_f/\epsilon_\alpha \simeq 6.4$. Then applying heating power p_H results in extra heating power

$$\Delta P \simeq p_H \left[1 + 6.4\,(\chi_\alpha + 2/\nu\tau) + \left(\frac{6.4}{M}\right)\left(\chi_\alpha + \frac{2}{\nu\tau} + 2\frac{\tau_\alpha}{\tau}\right)\right], \tag{18}$$

where the first term is the external heating power itself recovered in electron heat.

To continue this example for an ARIES-like design, suppose $M = 1$, i.e., it takes one watt to divert a watt. This means that the heating watt results in about 11/12 watts of increased α-particle power, or 5.9 total fusion watts. In addition, there is the extra watt of injected heat removed from electrons. Thus, using one heating watt in this manner results in 8+5.9+1=14.9 watts of heating power. This incremental "Q" of 14.9 is large enough to make a very worthwhile piggyback system for diverting power off of an operating reactor. Of course, should it be possible to divert more than one watt with one heating watt, the piggyback system is even more attractive. For example, if one watt could be diverted with just one half watt of external heating, then Q rises to 22.9 Note that just heating the ions, without diverting α-particle power, results merely in a piggyback Q of 6.9. (One should be cautious, however, in using the numbers in this example. These numbers are actually derived only in the limit of $\nu\tau \gg 1$, a limit that is only very marginally satisfied in the case here, so the numbers quoted in this example are not expected to be precise, and may be somewhat larger than for the cases where the operating point is closer to the optimum for fusion power density, i.e., $T \simeq 15$ KeV.)

6. Operating Point for Hot ion Mode

The results of the previous sections show that there is indeed significant incremental power gain in diverting α-particle power. This would suggest that an "add-on system" is highly desirable. What we do not know is whether the economic feasibility of the entire reactor is significantly improved; the add-on system may be very cost-effective in itself, but if it produces only a small fraction of the total reactor output, its impact on the cost of electricity will be marginal.

In this section we address the "maximal" problem; suppose that essentially all of the α-particle power can be diverted to fast ions, what kind of reactor can be built? Here, we assume that by means of this diversion we are in a "hot ion mode," where $T_i > T_e$. Moreover, as assumed by Clarke, we shall look for the benefits of operating in a regime such that $\tau_i \gg \tau_e$.

To assess these benefits, we shall use as a reference design a generic reactor that operates with $T_e \simeq T_i$, and in which there is a certain percentage of the reactor pressure taken up by the energetic α-particles. We shall look for a reactor design, in which the same pressure is confined as in the reference reactor, but in which there is significantly higher power density. Such a design, which may have comparable ion heat confinement times, but small electron confinement times, should achieve ignition in the hot ion mode, ideally with essentially no pressure taken up by energetic α-particles.

To find a self-consistent set of parameters, we first begin, again, with Eqs.(3), (4), and (8), which represent three linear equations, which we rewrite generalized to ions with arbitrary charge state ($\zeta \neq 1$) as

$$\beta_e = \frac{\nu\tau_e}{1+\nu\tau_e}\left\{\zeta\beta_i + \frac{1-\eta}{\nu}P_D\right\} \tag{19}$$

$$\zeta\beta_i = \frac{\nu\zeta\tau_i}{1+\nu\zeta\tau_i}\left\{\beta_e + \frac{\eta}{\nu}P_D\right\} \tag{20}$$

$$\beta_e + \beta_i = \beta, \tag{21}$$

where P_D is the total power that is deposited in the plasma, and where η represents the fraction of this power absorbed by the ions.

The power absorbed in the plasma is related to the α-particle power by

$$P_D = P_{\alpha D} + P_H, \tag{22}$$

where $P_{\alpha D}$ is the α-particle power that is absorbed and P_H is the external heating power. The power absorbed in the plasma ions might either be absorbed directly in the bulk of the fuel ion energy distribution, or it might first be absorbed in drawing out a nonthermal high-energy tail to this distribution, which then heats the bulk of the fuel ion distribution. In the latter case, there may be extra fusion power available, although there is a cost of some fast ion pressure. In the following, we assume that all the α-particle power diverted by waves, say $\eta_w P_{\alpha D}$, in the fast ion population. Also, we assume that a fraction η_{Hi} of

the external heating, or $\eta_{Hi}P_H$, is similarly deposited in fast ions. The available α-particle power can be written as

$$P_\alpha = c(T_i)\beta_i^2 f_D f_T + \eta_w P_{\alpha D}\chi_\alpha + \eta_{Hi}P_H\chi_\alpha, \tag{23}$$

where χ_α is the ratio of extra α-particle power produced by the the fast fuel ions to the amount of power diverted into these ions, and where f_D and f_T are the fractions of total ions taken up by deuterium and tritium respectively.

Equations (19), (20), and (21), can be solved for the three unknowns β_i, β_e, and P_D, resulting in

$$\frac{\beta_i}{\beta} = \frac{(1-\eta)\rho_i\rho_e + \eta\rho_i}{K}, \tag{24}$$

where, for convenience, we defined

$$\rho_i \equiv \frac{\nu\tau_i\zeta}{1+\nu\tau_i\zeta},$$

$$\rho_e \equiv \frac{\nu\tau_e}{1+\nu\tau_e},$$

$$K \equiv (1-\eta)\rho_e\zeta(1+\rho_i) + \eta\rho_i(1+\rho_e\zeta).$$

Note from Eq.(24) that β_i is maximized, i.e., $\beta_i \to \beta$, for $\eta \to 1$ and for $\rho_e \sim \tau_e \to 0$, irrespective of τ_i; in the event that $\eta \neq 1$, then β_i is maximized for $\tau_i \to \infty$, although, in this case, the maximum is less. Maximizing β_i means maximizing the thermal component of the fusion power through Eq.(23). Similarly, one can find β_e as

$$\frac{\beta_e}{\beta} = \frac{(1-\eta)\rho_e + \eta\rho_e\rho_i}{K/\zeta}, \tag{25}$$

The power necessary to maintain these plasma pressures is

$$\frac{P_D}{\nu\beta} = \frac{1-\rho_e\rho_i}{K/\zeta}. \tag{26}$$

Note that P_D increases as τ_e or τ_i decreases, since greater external power is needed if confinement is poor. However, for $\eta \to 1$, and $\rho_e \sim \tau_e \ll 1$, then $\beta_i \to \beta$, and the amount of external power necessary to maintain the ion and electron pressure, $P_D \to (\nu + \tau_i^{-1})\beta$, is essentially determined by the smaller of τ_i and $1/\nu$.

7. Ignition in the Hot ion Mode

Having achieved the parameters β_i and P_D for a given β and η, it is necessary to inquire whether these parameters require external heating ($P_H > 0$), or whether they obtain under ignited conditions ($P_H = 0$). In this section, we shall write an ignition criteria.

First, let us note some relations: If all the α-particle power is absorbed in the plasma, then $P_\alpha = P_D - P_H$. Let $P_H = \phi P_\alpha$. Then $P_D = (1+\phi)P_\alpha$.

Second, in writing a criteria for ignition, note that not all of the plasma pressure is available for fuel pressure; the most significant source of additional pressure, at least if the α-particle energy is not diverted, is the pressure from the hot energetic α-particles, $\beta_{\alpha H}$. Consider, however, that upon diverting this power to fast ions, there is then an increase in the fast ion pressure, so that the available bulk fuel pressure is

$$\beta = \beta_0 - \beta_{\alpha H} - \beta_{fi}, \tag{27}$$

where β_0 is the total available beta, and

$$\beta_{\alpha H} = (1-\eta_w)\tau_\alpha (P_D - P_H) = (1-\eta_w)\tau_\alpha P_D/(1+\phi), \tag{28}$$

$$\beta_{fi} = \eta_w \tau_s (P_D - P_H) + \eta_{Hi} P_H \tau_s = \eta_w \tau_s P_D/(1+\phi) + \eta_{Hi}\tau_s P_D \phi/(1+\phi), \tag{29}$$

where τ_α is the slowing down time of fast α-particles, and where where τ_s is the slowing down time of fast fuel ions (see Appendix A).

Note that the ratio of absorbed by the ions to power absorbed in the plasma is

$$\eta \equiv p_i/P_D = [\eta_w \eta_f P_{\alpha D} + (1-\eta_w)\eta_0 P_{\alpha D} + \eta_{Hi}\eta_f P_H]/P_D, \tag{30}$$

where η_f is the fraction of the power absorbed first by fast ions that is then absorbed by the bulk ions, and where η_0 is the fraction of α-particle power that collisionally is absorbed by ions in the absence of wave effects. This fraction depends, of course, on among other things, the electron temperature. Note that the fast α-particle pressure is proportional to $P_D - P_H$, the α-particle power dissipated in the plasma, since, by assumption, if there are any other α-particles generated, they are promptly lost, and the external heating power P_H does not contribute to the energetic α-particle pressure.

Using Eqs.(26), (27), (28), and (29), we find a reduction in the available pressure by

$$\beta = \frac{\beta_0}{1 + [(1-\eta_w)\tau_\alpha + \eta_w \tau_s + \phi \eta_{Hi}\tau_s]\nu\zeta(1-\rho_e\rho_i)/K} \equiv \frac{\beta_0}{G}. \tag{31}$$

Steady state operation is possible if $P_\alpha > P_D$. Alternatively, with all α-particle power deposited in the plasma ($P_\alpha = P_{\alpha D} = P_D - P_H$), one can write an expression for self-consistent burn, using Eq.(23), in the form

$$c\beta_i^2 f_D f_T = (1 - \eta_w \chi_\alpha - \phi \eta_{Hi}\chi_\alpha)\frac{P_D}{1+\phi}. \tag{32}$$

One would interpret Eq.(32) as an ignition criteria if $P_H = \phi = 0$. Using now Eqs. (24), (26), (31), and (32), one can write the self-consistent burn condition as

$$\frac{c_0\beta_0}{\nu} = \frac{G\zeta(1-\rho_e\rho_i)K}{[(1-\eta)\rho_e + \eta]^2 \rho_i^2 (1+\phi)}(1 - \eta_w\chi_\alpha - \phi\eta_{Hi}\chi_\alpha), \tag{33}$$

where the quantity G is defined from Eq.(31), and where we defined $c_0 \equiv c(T_i) f_D f_T$, which will be fairly insensitive to T_i in the range of interest.

One can take a number of useful and simplifying limits. First of all, in a pure D-T plasma, $\zeta = 1$. Let all the α-particle power be diverted, $\eta, \eta_w \to 1$, and assume no external heating, $P_H = \phi = 0$, i.e., ignition. Assume also negligible fast ion pressure, i.e., assume $\tau_s \to 0$. Then Eq.(33) simplifies to

$$c_0 \beta_0 \tau_i > (1 + \nu\tau_i)(1 - \chi_\alpha)(1 + \rho_e)(1 - \rho_e \rho_i). \tag{34}$$

One interesting question to ask is what τ_e (or ρ_e) minimizes the right-hand side (which is quadratic in ρ_e, assuming ν can be held fixed), of Eq.(34), and so makes ignition easier to achieve. The maximum of the right-hand side of Eq.(34), as a function of ρ_e, occurs at $\rho_e = (1 - \rho_i)/2\rho_i$, and the minima occur for $\rho_e \to \pm\infty$. With the restriction that $0 < \rho_e, \rho_i < 1$, it is clear that the minimum must occur at either of the end points of this region, namely, either at $\rho_e = 1$ or at $\rho_e = 0$. Moreover, for $\rho_i < 1/2$, namely poor ion heat confinement, the minimum occurs at $\rho_e = 0$ (poor electron heat confinement); and for $\rho_i > 1/2$, namely good ion heat confinement, the minimum occurs at $\rho_e = 1$ (good electron heat confinement). One must keep in mind, however, that $\nu\tau_e \to 0$ must occur for this to happen, however, for $\eta \to 1$ and $\tau_e \to 0$, then ν tends to be large (for fixed T_i).

The second of these statements is intuitive; when the ion heat confinement is very good, ignition occurs most easily also with good electron heat confinement. In the opposite limit, however, the result is not intuitive; here, when ion confinement is not very good, ignition is actually more easily achieved with poorer electron confinement, so long as all the α-particle power is diverted! The reason for this somewhat odd looking result is that although ion heat confinement is poor, poor electron heat confinement assures that at least $\beta_i > \beta_e$, i.e., operation in the hot ion mode.

To explore these ideas further, let us take three limits of Eq.(34): First, for $\rho_e \to 1$, the electron heat is very well confined and the ignition criteria reduces to

$$c_0 \beta_0 \tau_i > 2(1 - \chi_\alpha). \tag{35}$$

Second, suppose $\tau_i = \tau_e \equiv \tau$. Then, Eq.(34) reduces to

$$c_0 \beta_0 \tau > (1 - \chi_\alpha) \left(\frac{1 + 2\nu\tau}{1 + \nu\tau} \right)^2 \to 4(1 - \chi_\alpha), \tag{36}$$

where, the limit taken is for $\nu\tau \gg 1$. In this limit, where the confinement of both ion heat and electron heat is very good, the advantage in ignition margin of diverting α-particle power is (see Eq.(40) below) left to just two terms, the factor $1 - \chi_\alpha$, since the only nonthermal feature is the hot ion population, and the lack of fast α-particle pressure.

Consider now a third case of very poor electron heat confinement, ρ_e, $\tau_e \to 0$. The ignition criteria reduces to

$$c_0 \beta_0 \tau_i > (1 + \nu\tau_i)(1 - \chi_\alpha), \tag{37}$$

which, interestingly, gives a more relaxed ignition criteria than does the limit of good electron confinement (Eq.(35), provided that $\nu\tau_i < 1$, or, equivalently, $\rho_i < 1/2$. This is interesting because poorer confinement of the ion heat makes ignition easier. Additionally,

apart from the purely mathematical considerations that lead to the more relaxed ignition condition, it may in practice be hard to achieve the limit of very good electron heat confinement, whereas poor confinement can be arranged in a variety of ways.

These ideas can be put in perspective by considering the case of undiverted α-particle power $\eta_w = 0$, and, moreover, take the limit $\eta = 0$ (large T_e), in which limit, again with the assumptions of a D-T mixture ($\zeta = 1$) and ignition ($\phi = 0$), Eq.(33) reduces to

$$\frac{c_0\beta_0}{\nu} > \frac{1-\rho_e\rho_i}{\rho_e^2\rho_i^2}\left(\rho_e(1+\rho_i) + \nu\tau_\alpha(1-\rho_e\rho_i)\right). \tag{38}$$

First note a qualitative difference: here, in contrast to the case of diverting all the α-particle power, in the limit $\tau_e \to 0$ and when no α-particle power is diverted, there is no ignition possible.

Consider now the other cases: In the limit of very good electron heat confinement, $\tau_e \to \infty$, then $\rho_e \to 1$, and we require

$$c_0\beta_0\tau_i > 2 + \frac{1+\nu\tau_\alpha}{\nu\tau_i}, \tag{39}$$

which is more stringent than the condition for $\eta \to 1$, Eq.(35). For the third case, namely the limit $\tau_e = \tau_i \equiv \tau$, Eq.(38) reduces to the usual "$nT\tau$" ignition criteria in the form

$$c_0\beta_0\tau > \left(2 + \frac{1}{\nu\tau}\right)^2\left(1 + \frac{\tau_\alpha}{\tau}\right) \to 4(1+\tau_\alpha/\tau), \tag{40}$$

where the limit is taken for $\nu\tau \gg 1$ and this "normal" case may be compared to that obtained upon diverting power, under good confinement conditions, (see Eq.(36)).

Thus, whereas the diverting of the α-particle power always produces some advantage, it is in the case of very poor electron heat confinement that a qualitative difference emerges, making for a very different mode of operation, the so-called "hot ion mode," which is explored in the next three sections.

8. Optimizing Operation with Hot Ion Mode

A worthy goal in reactor design would be to find those operating conditions that maximize the fusion power density, yet keep the plasma ignited at constant plasma pressure. In this section we consider this optimization problem in the context of two limiting cases: normal operation with $T_e \simeq T_i$ and hot-ion operation with $T_e \ll T_i$.

Thus, to consider normal operation first, in the limit $T_e \simeq T_i$, with $\beta_e \simeq \beta_i = \beta/2$, maximize

$$P_\alpha = \epsilon_\alpha\frac{n^2\langle\sigma v\rangle}{4} = \epsilon_\alpha\left(\frac{2}{3}\right)^2\frac{\beta^2\langle\sigma v\rangle}{16\,T_i^2} \equiv \frac{\beta^2}{16}g(T_i), \tag{41}$$

subject to the ignition constraint of Eq.(33). If the constraint were met for any ion temperature, then P_α would simply be maximized when $g(T_i)$ is maximized with respect to T_i. This function has a well-known maximum at $T_i \simeq 15\,\mathrm{keV}$. Then, the density at optimal operation is found from $n = \beta/3T_i$.

The optimization in the presence of diverting α-particle power is considerably more complicated, since large temperature differences maximize the fusion power density but are hard to maintain. To proceed, use Eq.(23) with $P_D = P_\alpha$ at ignition, to write

$$P_\alpha = \frac{\beta^2}{16}\frac{1}{1-\eta_w\chi_\alpha}g(T_i)\frac{4}{(1+r)^2}, \tag{42}$$

where $r = r(\rho_e, \rho_i, \eta)$ is the ratio of electron to ion temperature, which can be found from Eqs.(24) and (25) as

$$r \equiv \frac{T_e}{T_i} = \frac{\rho_e}{\rho_i}\left[\frac{1-\eta+\eta\rho_i}{(1-\eta)\rho_e+\eta}\right]. \tag{43}$$

Note the critical role played by diverting α-particle power: for $\eta \to 0$, $r \to 1/\rho_i > 1$, meaning that a hot ion mode is not obtainable; on the other hand, note that for $\eta \to 1$, $r \to \rho_e < 1$, meaning that a hot ion mode is not only obtainable, but can be made arbitrarily large, in principle, simply by spoiling the electron heat confinement

Note also that the ignition condition, Eq.(33), for an optimized operating point at $P_\alpha = P_D$, can be in the form $H(\rho_e, \rho_i, \eta, \nu) = 0$. The electron-ion temperature equilibration rate ν can be written in the form

$$\nu = a\beta\frac{1}{T_i^{5/2}(1+r)r^{3/2}} = \nu(r, T_i), \tag{44}$$

where the constant a depends on the impurity content. Maximizing P_α is thus reduced to a maximization over the parameters $(T_i, \rho_i, \rho_e, \eta)$, with one constraint.

Each of these parameters may be treated independently; for example, ρ_e is monotonic in τ_e, which is considered here as a free parameter. The optimization of P_α over η and ρ_i (or τ_i) is straightforward, since it is always preferred to divert more energy into the fast ions and to contain the ion heat longer. Thus, to maximize P_α, separately maximize η and ρ_i, i.e., take η and ρ_i at the maximum practically obtainable values. (Note, however, that in the limit $\eta \to 1$, the optimization is sensitive to η, but only weakly sensitive to ρ_i.) Then, the ignition condition can be used to write, e.g., ρ_e and hence r in terms of T_i, so that P_α can be written as a function of T_i only. Note, however, that maximizing P_α with respect to T_i may now occur at temperatures other than 15 keV. The foregoing procedure demonstrates that the optimization problem in the limit of the hot ion mode is well posed and will yield a definite set of optimized parameters.

To illustrate this procedure in a limit of interest, consider the case $\zeta, \eta, \eta_w \to 1$. For simplicity, also choose $\tau_s = 0$. In this limit, $\beta \to \beta_0$, $\beta_e/\beta_i = r \to \rho_e$, and $K \to \rho_i(1+\rho_e) = \rho_i(1+r)$. The ignition condition (34) can then be written as

$$c\beta_0/\nu = (c\beta_0/a)T_i^{5/2}(1+r)r^{3/2} = (1-\chi_\alpha)(1+r)(1-r\rho_i)/\rho_i, \tag{45}$$

from which one has $r = r(T_i; \rho_i)$ as a monotonically decreasing function of T_i, with ρ_i entering, not particularly sensitively, as a parameter. Note, in Eq.(42), that for $T_i > 15\,\mathrm{KeV}$, $g(T_i)$ is monotonically decreasing, whereas $(1+r)^{-2}$ is monotonically increasing in T_i. Hence, as a function of T_i, there is a single maximum to P_α satisfying ignition,

although not necessarily at $T_e = T_i = 15\,\mathrm{KeV}$. For example, if the factor $1 - \chi_\alpha$ in Eq.(45) becomes small, it is clear that r can become small and then P_α will be maximized (at considerably greater power density than for normal operation) at $T_i = 15\,\mathrm{KeV}$ but $T_e \ll 15\,\mathrm{KeV}$.

9. Examples of Ignition Parameters

In this section, we present examples in which the fusion power density is significantly increased by diverting α-particle power. To establish a comparison, let us consider a reference reactor with about the following parameters at ignition in the absence of diverting the α-particle power: $T_e \simeq T_i = 20\,\mathrm{keV}$, $n_e = n_i = 1.2\,10^{14}\,\mathrm{cm}^{-3}$, and $\tau_e = \tau_i = 2.5\,\mathrm{s}$. Taking $Z_{\mathrm{eff}} = 1$, i.e. assuming a nearly pure hydrogen plasma, implies $\nu\tau_e = \nu\tau_i \simeq 3$ and $\rho_e = \rho_i = 0.75$. This reactor is very similar to the ARIES-I design[12] (Final Design, p. 1-13, Vol 1., 1991), which ignites with these average parameters, except for additional heating of 100 MW for current drive power and an effective ion charge state $Z_{\mathrm{eff}} = 1.65$. Note that in this reactor the fast alpha particle pressure is about 1/6 the plasma pressure. This reactor delivers about 2 GW fusion power. This reference reactor must be made more precise, which we do below, in order to be sure that the parameters specified are indeed self-consistent at ignition.

We inquire now as to whether substantially more fusion power can be produced under the constraint that the total plasma pressure remain constant. So long as a substantial fraction of the α-particle power can be diverted, we shall show that for a variety of settings a reactor with about twice the fusion power density is possible. Note that this means that confinement times will tend to be shorter; after all, if $P_f \sim nT/\tau$ at ignition (where n, T, and τ are an unspecified generic density, temperature and confinement time), then if nT must remain constant while P_f doubles, then clearly τ must be halved. In the following cases, we solve self-consistently for the plasma parameters at ignition by choosing T_i and T_e, and then finding all the other parameters at fixed total pressure of the plasma.

Table 1 establishes the comparison. Here, the total plasma pressure and the electron and ion temperature correspond roughly to the ARIES-I reactor, but without impurities, and without any external power (ϕ=0) being deposited for current drive. The fraction of the total power deposited in ions, η, is not identically zero because α-particles do slow down somewhat on ions. The self-consistent solution to the 0-D equations gives P_f of 4.7 Watts/cm^3 without blanket reactions. In order to arrive at electrons and ions at the same temperature, the electron confinement time must be half the ion confinement time. Note that this is consistent with α-particle heating on the electrons twice that on the ions. The fast alpha particle pressure accounts for 18 percent of the total plasma pressure. Recall that, throughout this paper, τ_e lumps both the effects of radiation by synchrotron motion or bremsstrahlung, and the effects of heat conduction or convection. (This is a somewhat different convention than what is generally followed in the literature.)

These reactor parameters do not optimize for the fusion power density; rather, the temperature is chosen at 20 KeV, which is high, to accomodate high current drive efficiency. A reactor design at the same pressure as ARIES-I that would optimize for fusion power density is shown in Table 2. Here, $T_i = T_e$=15 KeV, which is close to the maximum reactivity per unit pressure of the plasma, and, in addition, the α-particles slow down more rapidly on the colder denser plasma, so that the fusion power density, P_f, increases

by 30%.

Now let us consider the possibilities for increased fusion power density if 3/4 of the α-particle power can be diverted to the fast ions: Table 3 shows that this diversion makes possible a very different regime of operation, in which T_i is nearly twice T_e, $\tau_e \ll \tau_i$, and P_f is 2.2 times higher in this case than in Table 1. This increase is due to the increase in the ion pressure that is available in the hot ion mode of operation, to the reduction in the fast α particle pressure, and to an increase in the reactivity due to the creation of a fast deuterium tail. Note that the reduction in fast α pressure arises from two effects: first, there is the instantaneous and direct diversion of 3/4 of the α-particle energy to ions, and, second, the 1/4 of the α-particles that are not directly affected, now slow down much faster because the electron temperature is halved. Note also that, interestingly, the electron confinement time is almost 3 times shorter than for the reference case and is only 1/6 of the ion heat confinement time.

Table 4 shows a somewhat different ignition regime also made possible by diverting the α-particle power. Although the temperature disparity between electrons and ions is less than that shown Table 3, the fusion power density is about the same. While the relative pressure taken up by the ions is necessarily less than that in Table 3, operation at 15 KeV for the ions is more efficient use of the available ion pressure. This scenario accomodates a lower ion heat confinement time; although τ_e is longer, τ_i is almost half the τ_i in Table 3. In fact, in Table 3, $\tau_i/\tau_e = 5.9$, while, in Table 4, $\tau_i/\tau_e = 1.8$. In any event, what these tables show is that fusion power densities in excess of twice the reference design for ARIES-I (Table 1), are clearly attainable. Power densities about 1.6 the optimized reference design (Table 2) are also attainable, but in the optimized reference case, the optimization is just for power density, without any provision for current drive.

Tables 1 through 4 represent cases without external heating, and with no impurities present in the plasma. In the following, these additional effects are taken into account in a number of tables that represent plasma parameters under self-consistent burn, rather than ignition. In Table 5, these parameters are calculated taking into account impurities characteristic of the ARIES-I design (Z_{eff}=1.65). External heating (100 MW or Q=20) is also similar to the ARIES-I-like reference design given in Table 1. The external heating, equal to a quarter of the α particle power, is deposited in the electrons, simulating the effect of the ARIES-I ICRF current drive. Note that the fusion power is now considerably smaller, and the ion heat confinement time that is necessary to reach self-consistent burn is considerably larger. The fraction of power going to the ions, η, has decreased because the external heating is to the electrons. On the other hand, the fast α-particle pressure is decreased, both because there are fewer α-particles at the reduced level of fusion power, and because the α-particles that remain slow down faster as they collide aginst the higher background density of electrons.

Tables 6 and 7 show that, if 3/4 of the α-particle power can be diverted to the ions, the fusion power density still increases by a factor of about two. Table 6 shows over a factor of two greater fusion power density than that given in Table 5, for the case when the same percentage of α-particle power is injected into the plasma through external heating (Q=20). In these cases the external heating is delivered to the ions; presumably this heating is amplified by the α-particles. The current drive is presumably

accomplished concommitantly; after all, with so much rf power delivered to the ions, even a relatively inefficient form of ion current drive[13,14] would deliver sufficient toroidal current. Table 7 describes the case Q=40, where the same absolute amount of external heating is employed, even though the reactor delivers twice the fusion power output. For this example, it was assumed that 3/4 of the energy is extracted from all of the α-particles, rather than all of the energy extracted from 3/4 of the α-particles. There is some advantage in in extracting power in this manner. Note that the effect of the impurities is to make temperature differences between ions and electrons more difficult to sustain, both because the equilibration rate is increased, and because the lower fusion power densities provides less of a drive. The effect of external heating on the ions has the opposite effect, making more power available to sustain temperature differences between electrons and ions.

These reference cases, and the comparison cases when 3/4 of the α-particle power can be diverted, show that, in a variety of settings, double the fusion power density is attainable through diverting the α-particle power.

10. Self-consistent Burn Plots

It is very valuable to depict graphically how the operating point at ignition can be chosen to optimize the fusion power density. It turns out that a very useful method of display occurs by plotting contours of various plasma parameters as a function of ρ_e and ρ_i. For example, the fusion power density is given from Eq.(42), for a given pressure, for a given fraction η of diverted power, and for a given χ_α in terms of r and T_i. However, r can be written from Eq.(43) in terms of ρ_e and ρ_i. Then the ignition condition, Eq.(33), with the help of Eq.(44), can be used to find T_i also in terms of ρ_e and ρ_i.

In the following, we specify values for β_0, η, η_w, and χ_α, as well as any details of the impurities present or the external heating. Then we find the ion temperature T_i that solves for equilibrium burn, or what we call ignition in the event of no external heating. Then, given T_i, ρ_e and ρ_i, it is possible to solve for quantities such as P_f, T_e, τ_i, and τ_e. Incidentally, it is by no means assured that a solution, i.e. a set of self-consistent burn parameters, exists for the complete range of ρ_e and ρ_i; in fact, it turns out that ignition is generally not possible for $T_i > 80$ KeV. Since we solve directly for T_i, it is most convenient numerically simply not to attempt a solution in this region and, in the figures, this region has been shaded out.

For illustration, consider Fig. 1a, which shows contours of the fusion power density, P_f, for the case of ARIES-I-like parameters, with no diversion of α-particle power. Note that the maximum fusion power density is in the range of 7 W/cm^3, and it occurs for $\rho_i \to 1$, but for ρ_e considerably different from 1. The shaded area corresponds to $T_i > 80$ KeV. In Figs. 1b–1e, additional parameters are plotted in terms of ρ_e and ρ_i. Note that from Fig. 1b, it is clear that solutions must be possible in the full region $T_i < 80$ KeV, although the parameters that satisfy the solution may be unrealistic and correspond to extremely low fusion power density. Corresponding to the maximum fusion power density is T_i between 10 and 15 KeV, as one might expect. Now let us inquire as to the other parameters near the fusion power maximum. From Fig. 1c, it is clear that this maximum is also characterized by T_e between 10 and 15 KeV, which is not an unexpected result. However, from Figs. 1d and 1e, one sees that the maximum fusion power density requires $\tau_i \to \infty$, with $\tau_e \to 0$. This indicates that even in a conventional fusion reactor, i.e., with

no diverted α-particle power, there is an advantage in small electron heat confinement times.

Note that the fusion power is maximized here for T_i about equal to or somewhat greater than T_e. These hot-ion modes of operation, although not very pronounced, are available even though no α-particle power is diverted and only about 28% naturally goes to the ions. What enables these modes of operation is short electron heat confinement times, something that forseen above through analytic considerations. In these ignition modes, there is little sensitivity to the precise value of the ion heat confinement, since most of the ion heat is lost through the electron channel rather than by direct means. As the electron heat confinement times increase, at constant ion heat confinement times, the fusion power density decreases as more of the plasma pressure is taken up by the electrons. The sensitivity on the electron confinement time is quite dramatic; for example, consider operating points in the vicinity of ion heat confinement times of about 2 s and electron heat confinement times of about 1 s. Changing the ion heat confinement times moves the operating point roughly along contours of constant fusion power density, whereas changing the electron heat confinement times moves the operating point roughly perpendicular to contours of constant fusion power density. For example, at $\tau_i = 2.5\,\mathrm{s}$ and $\tau_e = 1\,\mathrm{s}$, results in ignition at $P_f = 4\,\mathrm{Wcm}^{-3}$, but at the same τ_i, with $\tau_e = 0.6\,\mathrm{s}$ results in ignition at $P_f = 7\,\mathrm{Wcm}^{-3}$. Of course, if the electron heat confinement time is too small, then there may be no ignition point at all. Hence, in optimizing reactor performance, one must design for adequate electron heat confinement. However, more than the adequate amount for ignition is actually deleterious to the reactor performance.

There are several other features of Figs. 1a–1e that are worth pointing out. Let us inquire how ignition is possible in the corners of the ρ_e–ρ_i domain. Consider first the lower left corner and the lower right corner. In both of these cases the fusion power density is very low, but the ion heat confinement and the electron heat confinement times must be very large. The lower left corner corresponds to large ion and electron temperatures, but very small densities. The lower right corner corresponds to large electron temperatures, but small ion temperatures. These cases illustrate that ignition at very low power density is possible if confinement times are long enough; indeed, even a glass of water can be considered to be ignited (absent evaporation) in the sense that the fusion power though uninterestingly small can exceed the power required to confine the fuel.

Somewhat more interesting is the upper right corner, where both T_i and T_e are modest and about equal, and which can be reached at modest values of τ_e and τ_i. (This is close to the present ignition scenario on the ITER tokamak, where confinement times are several seconds, and ion and electron temperatures are about equal and in the range of 10 KeV.) Note, however, that this regime, while not at the very low power densities characteristic of operation in the lower corners of the ρ_e–ρ_i domain, still tends to be off the maximum fusion power density, even in the case here in which no power is diverted.

The difference between the upper right corner and the lower left corner is that the temperatures tend to decrease towards the upper right corner, hence, at constant pressure, the densities tend to increase. That leads to close collisional coupling between the electrons and ions, so the electron and ion temperatures tend to become equal in the upper right corner. The lower left corner supports greater differences between the ion and electron

temperatures. The fusion power maximum, however, is reached with some finite, if not dramatic, temperature differences.

In Fig. 2a, we show that much higher fusion power densities are possible when 75% of the α-particle power is diverted to deuterium ions at 70 KeV. The highest contour level shown is 12 MWcm^{-3}, which can be compared to the contour level at 7 MWcm^{-3} in Fig. 1a, when no power is diverted by waves. Immediately evident from Fig. 2a, in comparison to Fig. 1a, is that there is a shift of the fusion power density contours to lower ρ_e. Similarly, the maximum power density occurs at lower ρ_e, which corresponds, as we expect now, to lower electron heat containment. From Fig. 2b, in comparison to Fig. 1b, it is evident that the fusion power maximum occurs at higher ion temperature, between 15 and 20 KeV, in the case of diverting α-particle power. One can see from Fig. 2c, why there is that shift to higher ion temperature; it is only the higher ion temperatures that allow higher electron temperatures, while still retaining the preponderance of the pressure in ions. The higher electron temperatures are necessary to achieve smaller collisional coupling between the ions and electrons.

If one were to overlay Fig. 2d and Fig. 2e, it would become clear what pairs of τ_e and τ_i are consistent with ignition. Note in particular that at a constant τ_i, there is a minimum τ_e necessary for there to be overlap anywhere. However, for τ_e greater than this minimum value, there is, in general, a monotonic decrease in fusion power density with increasing τ_e.

It ought to be pointed out that, in constructing these contour plots, certain approximations were made for convenience. The quantities η, $\nu\tau_\alpha$, and χ_α are rather complicated implicit functions of T_e and T_i that are difficult to solve for even numerically. Thus, for simplicity, these quantities were taken to be constant, so that at one ignition point, i.e., for one pair of values T_e and T_i consistent with ignition, these quantities are exactly given. In practice, within the regimes of interest, the quantities η, $\nu\tau_\alpha$, and χ_α are not strongly varying at all as functions of the temperatures, so that taking these quantities as constant is an approximation that is not significant. If more accuracy were necessary, these contour plots could be improved to arbitrary precision through an iterative procedure. In any event, the tables given in Sec. 8 are entirely consistent and can be used to justify this approximation. Fig. 1 is precisely self-consistent for $T_e = 15$ KeV (Table 2), whereas Fig. 2 is precisely self-consistent for $T_i = 20$ KeV and $T_e = 12$ KeV (Table 3).

Note that the fusion power density scales with β^2, the available plasma pressure squared. Thus, to calculate operation at say twice the plasma pressure, scale the the fusion power density by four at each point in ρ_e-ρ_i space. To remain at the same point in ρ_e-ρ_i space, for example, near the maximum, the densities can all be scaled up by two and the confinement times can all be scaled down by two, so that the slowing down times decrease by a factor of two, but the fraction of the pressure taken up by the hot α-particles remains the same. With only the above scalings, the optimum operating points then remain at the same temperatures for both the electrons and ions.

In Figs. 3 and 4, it is shown that very similar conclusions, namely about a factor of 2 increase in the fusion power density, can be reached in the case of external heating and impurities. In Fig. 3, we take the effective ion charge state to be $Z_{\text{eff}} = 1.65$, and we assume that external heating, $\phi = 0.25$, corresponding to about 100 MW, is applied

to support the current drive. This is consistent with the more precise ARIES-I scenario. In Fig. 4, with 75% diversion of the α-particle power, we take the same ion charge state and circulating power fraction, but here the external heating is applied to the ions. It is assumed also that the current drive is sustained by the external heating amplified by the α-particles through some form of ion current drive. What these figures illustrate is that the relative advantage of diverting the α-particle power remains about the same, even as the absolute fusion power densities attainable decrease in the presence of impurities.

11. Diverting energetic α-particle and Proton Power in D-He^3 Reactors

The utility of operting at higher fusion power density by diverting power from energetic fusion charged byproducts is particularly important in advanced fuel reactors such as D-He^3. Consider, for example, the ARIES-III reactor, operating at about $T_e = T_i = 55$ KeV.[15] Here 70% of the fusion power output is promptly radiated by electrons. The salient parameters for this reference reactor are shown in Table 8, where we have assumed no impurities and no external heating. Note that the proton pressure is significantly more important than the α-particle pressure, both because the protons are born with more energy and because the protons slow down more slowly.

In Table 9, the result of diverting 75% of the fast ion power is shown. This power is diverted both from the α-particles and from the proton byproducts of the D-He^3 fusion. The power is diverted to deuterium at 350 KeV. Through diverting this power, a temperature difference between the ions and the electrons can be sustained, so that more than double the fusion power density is then obtained. The increased power density is due in a large part to the decrease in the fast proton pressure that occurs both because of the diverting of the power and because of the increased collisionality. The increase in the collisioality arises from both the reduction in the electron temperature and the background density increase in ions and electrons that is now possible under constant pressure operation. In order to show the effect of diverting power to the bulk of the ion distribution rather than to the energetic tail, we explore in Table 10 the result of diverting 75% of the charged fusion byproduct power to the bulk ions rather than to the tail deuterium ions. This reduces the fusion power by about 10%.

One further thing to bear in mind in examining the implications for D-He^3 reactors is that there is considerable doubt at present about how the hoped-for operating parameters might be achieved in these devices. For example, there are assumptions in the ARIES-III design that very high plasma pressures can be contained within the tokamak. There are also assumptions about the radiation of the very hot electrons, including how this radiation might be reflected back into the plasma. It may turn out that radiative transport of electron heat dominates the electron heat losses so that, effectively, very low τ_e can not be avoided in the conventional designs. If that turns out to be the case, then diverting energetic α-particle and proton power to ions will be even more important, because any power going into electrons will be effectively lost. If τ_e is very small, then unless power can be diverted, there may be no ignition possible at all. By diverting power, not only is the fusion power density increased to sustain the self-consistent burn, but the tokamak may be operated at lower electron temperatures where radiation and radiative transport will be manageable.

12. Summary and Conclusions

In posing the question of the utility of extracting α-particle power, and diverting this power to fast ions, it was useful to consider separately an incremental and a maximal problem. In the former, the reactor conditions do not vary, and a small add-on system was shown to have large power multiplication possibilities. In the latter posing of the problem, power densities of about twice that achievable in normal operation were shown for a variety of cases. These cases represent possibilities in reactor operation, rather than completely optimized parameters, although by means of contour plots in ρ_e-ρ_i space, it can be seen how one might optimize the power density, or other parameters, at constant pressure. Characteristic of high power density reactors is substantial diversion of α-particle power and low electron energy confinement time.

It was necessary to exercise care in the posing of the problem: after all, there must in any event be a burn control to write equations with steady state solutions. In addition, as power is diverted to fast ions and then to ions, a number of effects come into play, as the relative amounts of pressure taken up by electrons, fuel ions, and fast α-particles shift.

One effect that has not been incorpoorated in the considerations here is the depletion of α-particle ash, i.e., even the thermalized α-particles, that generally accompanies methods of channeling the α-particle power. The depletion of the ash would arise because in extracting the free energy of the α-particles, waves tend to diffuse α-particles to the tokamak periphery.[9] To the extent that the thermal ash is removed from the reactor by means of diverting the α-particle power, the reactor power density would be improved even further than the factor of 2 reported in this paper. This is an effect that is particularly important for the case of advanced fuels, such as D-He^3, where there is both a tendency for greater accumulation of thermal ash, and a greater urgency to make use of all the available plasma pressure.

This work concludes that a reactor operating at much higher power densities is possible, particularly as the electron energy confinement time decreases. Such a reactor is far more interesting economically than could be contemplated in the absence of diverting α-particle power. It could be smaller, the magnetic field could be reduced, and, in principle, since there is less free energy in the energetic α-particle distribution, the plasma is less prone to deleterious instabilities or disruptions that might have been destabilizedby the energetic α-particles.. The additional power required to divert the α-particle power could also secure the burn control, and, in principle, augmented by the diverted α-particle power, drive entirely the toroidal plasma current.

The enhanced fusion power density is also available upon diverting energetic charged fusion byproducts in D-He^3; in fact, the possibilities in diverting power are particularly important in fuel mixtures such as D-D, or D-He^3 where serious economic consideration will depend upon the attainment of higher fusion power densities.

Acknowledgements

The authors are indebted to Dr. David Mikkelsen and Dr. Harold Furth for very useful, stimulating, and insightful comments. In particular, the authors benefited greatly from the invariably correct predictions and intuition of Dr. Mikkelsen. The authors also acknowledge very useful discussions with Mr. Phil Snyder on the topic of enhanced re-

activity of nonthermal distributions. Much of this work is an outgrowth of joint work of Dr. Jean-Marcel Rax and one of the authors (NJF), and his influence on the present work is gratefully acknowledged. This work was supported by the United States Department of Energy under contract number DE–AC02–76–CHO3073. One of the authors (MCH) acknowledges the support of the Fannie and John Hertz Foundation.

References

1. J. M. Dawson, H. P. Furth, and F. H. Tenney, Phys. Rev. Lett. **26**, 1156 (1971).
2. H. P. Furth and D. L. Jassby, Phys. Rev. Lett. **32**, 1976 (1972).
3. D. L. Jassby, Nucl. Fusion **17**, 309 (1977).
4. J. G. Cordey and F. A. Haas, in Plasma Physics and Controlled Nuclear Fusion Research (Proc. 6th Int. Conf. on Plasma Phys. and Controlled Thermonuclear Fusion, Berchtesgaden, 1976) Vol. 2, IAEA, Vienna, 423 (1977).
5. J. F. Clarke, Nucl. Fusion **20**, 563 (1980).
6. L. A. Berry, C. E. Bush, J. D. Callen, R. J. Colchin, J. L. Dunlap et al., in Plasma Physics and Controlled Nuclear Fusion Research (Proc. 6th Int. Conf. on Plasma Phys. and Controlled Thermonuclear Fusion, Berchtesgaden, 1976) Vol. 2, IAEA, Vienna, 49 (1977).
7. TFR Group, in Plasma Physics and Controlled Nuclear Fusion Research (Proc. 6th Int. Conf. on Plasma Phys. and Controlled Thermonuclear Fusion, Berchtesgaden, 1976) Vol. 2, IAEA, Vienna, 69 (1977).
8. H. Eubank, R.J. Goldston, V. Arunasalam, M. Bitter, K. Bol, et al., in Plasma Physics and Controlled Nuclear Fusion Research (Proc. 7th Int. Conf. on Plasma Phys. and Controlled Thermonuclear Fusion, Berchtesgaden, 1978) Vol. 1, IAEA, Vienna, 167 (1979).
9. N. J. Fisch and J. M. Rax, Phys. Rev. Lett. **69**, 612 (1992).
10. N. J. Fisch and J. M. Rax, Phys. Fluids B **5**, 1754 (1993).
11. N. J. Fisch and J. M. Rax, in Plasma Physics and Controlled Nuclear Fusion Research (Proc. 14th Int. Conf. on Plasma Phys. and Controlled Thermonuclear Fusion, Würzburg, 1992) IAEA, Vienna, Vol. 1, 769 (1993).
12. The ARIES-I Tokamak Reactor Study, Final Report, Vols. 1 and 2, UCLA Report UCLA-PPG-1323 (1991).
13. N. J. Fisch, Nucl. Fusion **24**, 371 (1984).
14. N. J. Fisch, Rev. Mod. Phys. **59**, 175 (1987).
15. C. G. Batheke, K. A. Werley, R. L. Miller, R. A. Krakowski, and J. L. Santarius, in Proc. 14th IEEE/NPSS Symposium on Fusion Eng., IEEE, N.J., Vol. 1, 219 (1991).

Appendix A. Nonthermal Reactivity and Pressure

In this appendix we compute χ_α, the fraction of power diverted to superthermal fuel ions that is recovered as α-particle power through the enhanced tail fusion reactivity. Apart from the power cost in producing the nonthermal distribution of fuel ions, there is also a pressure cost, since these fast ions (and the electrons required to neutralize them—but that is a small term) take up a certain amount of the plasma pressure that is then not available to thermal ions and electrons.

Suppose a nonthermal distribution of ions at a given energy in addition to a thermal distribution of ions and electrons. Assume that the number of particles in this nonthermal distribution is small compared to the number of ions. The α-particle power produced by these ions is

$$P_\alpha = \epsilon_\alpha n_f n_T \int \sigma(\mathbf{v}_T - \mathbf{v}_f)|\mathbf{v}_T - \mathbf{v}_f| f_T(\mathbf{v}_T) d^3 v_T. \qquad (A1)$$

where n_f is the number density of fast ions, $\mathbf{v}_f$ is the velocity of the fast ions, and ϵ_α is 3.5 MeV. In this paper, the fast ions are chosen to be deuterium ions rather than tritium ions, for which a slightly larger χ_α should be available.

The amount of power necessary to maintain a nonthermal distribution of ions at a given energy E_d can be written as

$$P_{\text{input}} = n_f \nu_\epsilon(v) E_d, \qquad (A2)$$

where ν_ϵ is the energy slowing down rate for the fast ions. Hence, χ_α can be written as

$$\chi_\alpha \equiv \frac{P_\alpha}{P_{\text{input}}} = \frac{E_\alpha n_T \int \sigma(\mathbf{v}_T - \mathbf{v}_f)|\mathbf{v}_T - \mathbf{v}_f| f_T(\mathbf{v}_T) d^3 v_T}{\nu_\epsilon(v) E_d}. \qquad (A3)$$

In Fig. 5, we show how χ_α depends on both the energy of the fast ions and the background ion and electron temperatures; note, however, that χ_α is independent of the background density. The values given in this figure are for a 50:50 D-T mixture; for a tritium rich mixture, these values could be about doubled.

The extra pressure taken up by the fast ion distribution is just

$$\beta_{fi} = n_f E_d, \qquad (A4)$$

or, in terms of the power diverted,

$$\beta_{fi} = \frac{P_{\text{input}}}{\nu_\epsilon(v)}. \qquad (A5)$$

Note that the fast ions represent added deuterium to the plasma, so that it is only the ratio now of thermal deuterium to thermal tritium that is 50:50. Together with the added fast deuterium, to maintain charge neutrality, there must also be additional electrons added. These additional electrons, maintained at the electron temperature, cost in plasma pressure. This added electron pressure has been neglected in our calculations, since it is

small compared to the extra fast ion pressure which, in turn, is small compared to the overall pressure in the reactor.

It is worth pointing out that in practice it is not a δ-function distribution of particles that is maintained, rather there is a slowing down distribution that is maintained. The calculation of χ_α can also be posed in an incremental way[11], in which the incremental effect of heating on the slowing down distribution is calculated. However, it turns out that, because this distribution arises from the constant heating of ions at a specified energy that then slow down, both calculations yield the same result.

Table Captions

Table 1: Operating point based on the ARIES-I design.

Table 2: Operating point based on the ARIES-I design, except for $T_i = T_e$=15 KeV.

Table 3: Operating point based on the ARIES-I design, except for 75% of the α particle power diverted to fast deuterium ions at 70 KeV.

Table 4: Operating point based on the ARIES-I design, except for 75% of the α particle power diverted to fast deuterium ions at 70 KeV and $\tau_i/\tau_e \simeq 2$.

Table 5: Operating point based on the ARIES-I design, with impurities and external heating included (Q=20).

Table 6: Operating point based on the ARIES-I design, except for 75% of the α particle power diverted to fast deuterium ions at 70 KeV. Impurities and external heating are included (Q=20).

Table 7: Operating point based on the ARIES-I design, except for 75% of the α particle power diverted to fast deuterium ions at 70 KeV. Impurities and external heating are included (Q=40). Note, in this example, for comparison, 75% of the α-particle energy is diverted from 100% of the α-particles. In other words, here it is imagined that waves cool all α particles from 3.5 MeV to 875 KeV, rather than, as imagined in all the other examples in of this paper, that waves extract 100% of the α-particle energy from 75% of the α-particles.

Table 8: Operating point based on the ARIES-III design

Table 9: Operating point based on the ARIES-III design, except for 75% of the fusion product power diverted to 350 KeV deuterium ions.

Table 10: Operating point based on the ARIES-III design, except for 75% of the fusion product power diverted to bulk fuel ions.

Figure Captions

Figure 1.a: Contours of P_f versus ρ_e and ρ_i, with β_0=91, η=0.28, $\nu\tau_\alpha$=0.30. Contours from bottom to top are P_f (Watts/cm^3)=2, 3, 4, 5, 6, 7.

Figure 1.b: Contours of T_i versus ρ_e and ρ_i, with β_0=91, η=0.28, $\nu\tau_\alpha$=0.30. Contours from left to right are T_i (KeV)=40, 35, 30, 25, 20, 15, 10.

Figure 1.c: Contours of T_e versus ρ_e and ρ_i, with β_0=91, η=0.28, $\nu\tau_\alpha$=0.30. Contours from left to right are T_e (KeV)=40, 35, 30, 25, 20, 15, 10.

Figure 1.d: Contours of τ_i versus ρ_e and ρ_i, with β_0=91, η=0.28, $\nu\tau_\alpha$=0.30. Contours from left to right are τ_i (sec)=3.0, 2.5, 2.0, 1.5, 1.0.

Figure 1.e: Contours of τ_e versus ρ_e and ρ_i, with β_0=91, η=0.28, $\nu\tau_\alpha$=0.30. Contours from bottom to top are τ_e (sec)=3.0, 2.5, 2.0, 1.5, 1.0, 0.5.

Figure 2.a: Contours of P_f versus ρ_e and ρ_i, with β_0=91, η=0.69, η_w=0.75, χ_α=0.16, $\nu\tau_\alpha$=0.32. Diverted α particle power is applied to deuterium ions at 70 KeV. Contours from bottom to top are P_f (Watts/cm^3)=5, 6, 7, 8, 9, 10, 11, 12.

Figure 2.b: Contours of T_i versus ρ_e and ρ_i, with β_0=91, η=0.69, η_w=0.75, χ_α=0.16, $\nu\tau_\alpha$=0.32. Diverted α particle power is applied to deuterium ions at 70 KeV. Contours from left to right are T_i (KeV)=40, 35, 30, 25, 20, 15, 10.

Figure 2.c: Contours of T_e versus ρ_e and ρ_i, with β_0=91, η=0.69, η_w=0.75, χ_α=0.16, $\nu\tau_\alpha$=0.32. Diverted α particle power is applied to deuterium ions at 70 KeV. Contours from left to right are T_e (KeV)=40, 35, 30, 25, 20, 15, 10.

Figure 2.d: Contours of τ_i versus ρ_e and ρ_i, with β_0=91, η=0.69, η_w=0.75, χ_α=0.16, $\nu\tau_\alpha$=0.32. Diverted α particle power is applied to deuterium ions at 70 KeV. Contours from left to right are τ_i (sec)=3.0, 2.5, 2.0, 1.5, 1.0, 0.5.

Figure 2.e: Contours of τ_e versus ρ_e and ρ_i, with β_0=91, η=0.69, η_w=0.75, χ_α=0.16, $\nu\tau_\alpha$=0.32. Diverted α particle power is applied to deuterium ions at 70 KeV. Contours from bottom to top are τ_e (sec)=3.0, 2.5, 2.0, 1.5, 1.0, 0.5.

Figure 3.a: Contours of P_f versus ρ_e and ρ_i, with β_0=91, η=0.23, $\nu\tau_\alpha$=0.31. External heating with ϕ=0.25 is applied to the electrons. Impurities with Z_{eff}=1.65 are present. Contours from bottom to top are P_f (Watts/cm^3)=2, 3, 4, 5.

Figure 3.b: Contours of T_i versus ρ_e and ρ_i, with β_0=91, η=0.23, $\nu\tau_\alpha$=0.31. External heating with ϕ=0.25 is applied to the electrons. Impurities with Z_{eff}=1.65 are present. Contours from left to right are T_i (KeV)= 40, 35, 30, 25, 20, 15, 10.

Figure 3.c: Contours of T_e versus ρ_e and ρ_i, with β_0=91, η=0.23, $\nu\tau_\alpha$=0.31. External heating with ϕ=0.25 is applied to the electrons. Impurities with Z_{eff}=1.65 are present. Contours from left to right are T_e (KeV)=40, 35, 30, 25, 20, 15, 10.

Figure 3.d: Contours of τ_i versus ρ_e and ρ_i, with β_0=91, η=0.23, $\nu\tau_\alpha$=0.31. External heating with ϕ=0.25 is applied to the electrons. Impurities with Z_{eff}=1.65 are present. Contours from left to right are τ_i (sec)=3.0, 2.5, 2.0, 1.5, 1.0.

Figure 3.e: Contours of τ_e versus ρ_e and ρ_i, with β_0=91, η=0.23, $\nu\tau_\alpha$=0.31. External heating with ϕ=0.25 is applied to the electrons. Impurities with Z_{eff}=1.65 are present. Contours from bottom to top are τ_e (sec) = 3.0, 2.5, 2.0, 1.5, 1.0.

Figure 4.a: Contours of P_f versus ρ_e and ρ_i, with β_0=91, η=0.72, η_w=0.75, χ_α=0.12, $\nu\tau_\alpha$=0.33. Diverted α-particle power and external heating with ϕ=0.25 are applied to deuterium ions at 70 KeV. Impurities with Z_{eff}=1.65 are present. Contours from bottom to top are P_f (Watts/cm^3)=2, 3, 4, 5, 6, 7.

Figure 4.b: Contours of T_i versus ρ_e and ρ_i, with β_0=91, η=0.72, η_w=0.75, χ_α=0.12, $\nu\tau_\alpha$=0.33. Diverted α-particle power and external heating with ϕ=0.25 are applied to deuterium ions at 70 KeV. Impurities with Z_{eff}=1.65 are present. Contours from left to right are T_i (KeV)=40, 35, 30, 25, 20, 15, 10.

Figure 4.c: Contours of T_e versus ρ_e and ρ_i, with β_0=91, η=0.72, η_w=0.75, χ_α=0.12, $\nu\tau_\alpha$=0.33. Diverted α-particle power and external heating with ϕ=0.25 are applied to deuterium ions at 70 KeV. Impurities with Z_{eff}=1.65 are present. Contours from left to right are T_e (KeV)=40, 35, 30, 25, 20, 15, 10.

Figure 4.d: Contours of τ_i versus ρ_e and ρ_i, with β_0=91, η=0.72, η_w=0.75, χ_α=0.12,

$\nu\tau_\alpha$=0.33. Diverted α-particle power and external heating with ϕ=0.25 are applied to deuterium ions at 70 KeV. Impurities with Z_{eff}=1.65 are present. Contours from left to right are τ_i (sec)=3.0, 2.5, 2.0, 1.5, 1.0.

Figure 4.e: Contours of τ_e versus ρ_e and ρ_i, with β_0=91, η=0.72, η_w=0.75, χ_α=0.12, $\nu\tau_\alpha$=0.33. Diverted α-particle power and external heating with ϕ=0.25 are applied to deuterium ions at 70 KeV. Impurities with Z_{eff}=1.65 are present. Contours from bottom to top are τ_e (sec)=3.0, 2.5, 2.0, 1.5, 1.0, 0.5.

Figure 5: χ_α versus deuterium ion energy for a 50:50 D-T mixture, for $T_e \to \infty$, T_T = 0 KeV (dotted line); for T_e = 10 KeV, T_T = 0 KeV (dashed line); and for T_e = 10 KeV, T_T = 20 KeV (solid line).

$\beta_0(10^{14}\text{KeV/cm}^3)$	91.0
$T_i(\text{KeV})$	20.0
$T_e(\text{KeV})$	20.0
η	0.34
η_w	0
ϕ	0
ρ_i	0.65
ρ_e	0.49
$\nu(\text{sec})$	0.99
$\tau_i(\text{sec})$	1.86
$\tau_e(\text{sec})$	0.97
$n_i(10^{14}/\text{cm}^3)$	1.24
$n_e(10^{14}/\text{cm}^3)$	1.24
Z_{eff}	1.00
$P_f(\text{Watts/cm}^3)$	4.70
$\beta_{\alpha H}/\beta_0$	0.18
β_i/β_0	0.41
β_e/β_0	0.41
$\tau_\alpha(\text{sec})$	0.28

Table 1: Operating point based on the ARIES-I design.

$\beta_0(10^{14}\text{KeV/cm}^3)$	91.0
T_i(KeV)	15.0
T_e(KeV)	15.0
η	0.28
η_w	0
ϕ	0
ρ_i	0.81
ρ_e	0.61
ν(sec)	2.18
τ_i(sec)	1.89
τ_e(sec)	0.73
$n_i(10^{14}/\text{cm}^3)$	1.79
$n_e(10^{14}/\text{cm}^3)$	1.79
Z_{eff}	1.00
$P_f(\text{Watts/cm}^3)$	6.13
$\beta_{\alpha H}/\beta_0$	0.12
β_i/β_0	0.44
β_e/β_0	0.44
τ_α(sec)	0.14

Table 2: Operating point based on the ARIES-I design, except for T_i = T_e=15 KeV.

$\beta_0(10^{14}\text{KeV/cm}^3)$	91.0
$T_i(\text{KeV})$	20.0
$T_e(\text{KeV})$	12.0
η	0.69
η_w	0.75
ϕ	0
χ_α	0.16
ρ_i	0.84
ρ_e	0.48
$\nu(\text{sec})$	2.97
$\tau_i(\text{sec})$	1.83
$\tau_e(\text{sec})$	0.31
$n_i(10^{14}/\text{cm}^3)$	1.75
$n_e(10^{14}/\text{cm}^3)$	1.75
Z_{eff}	1.00
$P_f(\text{Watts/cm}^3)$	10.51
$\beta_{\alpha H}/\beta_0$	0.04
β_{fi}/β_0	0.04
β_i/β_0	0.58
β_e/β_0	0.34
$\tau_\alpha(\text{sec})$	0.11

Table 3: Operating point based on the ARIES-I design, except for 75% of the α-particle power diverted to fast deuterium ions at 70 KeV.

$\beta_0(10^{14}\text{KeV/cm}^3)$	91.0
$T_i(\text{KeV})$	15.0
$T_e(\text{KeV})$	12.0
η	0.69
η_w	0.75
ϕ	0
χ_α	0.16
ρ_i	0.77
ρ_e	0.66
$\nu(\text{sec})$	3.60
$\tau_i(\text{sec})$	0.95
$\tau_e(\text{sec})$	0.53
$n_i(10^{14}/\text{cm}^3)$	2.11
$n_e(10^{14}/\text{cm}^3)$	2.11
Z_{eff}	1.00
$P_f(\text{Watts/cm}^3)$	9.71
$\beta_{\alpha H}/\beta_0$	0.03
β_{fi}/β_0	0.03
β_i/β_0	0.52
β_e/β_0	0.42
$\tau_\alpha(\text{sec})$	0.09

Table 4: Operating point based on the ARIES-I design, except for 75% of the α-particle power diverted to fast deuterium ions at 70 KeV and $\tau_i/\tau_e \simeq 2$.

$\beta_0(10^{14}\text{KeV/cm}^3)$	91.0
T_i(KeV)	20.0
T_e(KeV)	20.0
η	0.28
η_w	0
ϕ	0.25
ρ_i	0.76
ρ_e	0.56
ν(sec)	1.20
τ_i(sec)	2.32
τ_e(sec)	1.05
$n_i(10^{14}/\text{cm}^3)$	1.23
$n_e(10^{14}/\text{cm}^3)$	1.44
Z_{eff}	1.65
$P_f(\text{Watts/cm}^3)$	3.64
$\beta_{\alpha H}/\beta_0$	0.12
β_i/β_0	0.41
β_e/β_0	0.47
τ_α(sec)	0.24

Table 5: Operating point based on the ARIES-I design, with impurities and external heating included (Q=20).

$\beta_0(10^{14}\text{KeV/cm}^3)$	91.0
T_i(KeV)	16.0
T_e(KeV)	11.7
η	0.72
η_w	0.75
ϕ	0.25
χ_α	0.12
ρ_i	0.92
ρ_e	0.64
ν(sec)	4.24
τ_i(sec)	2.27
τ_e(sec)	0.42
$n_i(10^{14}/\text{cm}^3)$	1.95
$n_e(10^{14}/\text{cm}^3)$	2.28
Z_{eff}	1.65
$P_f(\text{Watts/cm}^3)$	7.35
$\beta_{\alpha H}/\beta_0$	0.02
β_{fi}/β_0	0.03
β_i/β_0	0.51
β_e/β_0	0.44
τ_α(sec)	0.08

Table 6: Operating point based on the ARIES-I design, except for 75% of the α-particle power diverted to fast deuterium ions at 70 KeV. Impurities and external heating are included (Q=20).

$\beta_0(10^{14}\text{KeV/cm}^3)$	91.0
T_i(KeV)	17.0
T_e(KeV)	12.2
η	0.80
η_w	0.75
ϕ	0.13
χ_α	0.12
ρ_i	0.91
ρ_e	0.65
ν(sec)	3.83
τ_i(sec)	2.17
τ_e(sec)	0.49
$n_i(10^{14}/\text{cm}^3)$	1.87
$n_e(10^{14}/\text{cm}^3)$	2.19
Z_{eff}	1.65
$P_f(\text{Watts/cm}^3)$	7.39
$\beta_{\alpha H}/\beta_0$	0.01
β_{fi}/β_0	0.03
β_i/β_0	0.52
β_e/β_0	0.44
τ_α(sec)	0.04

Table 7: Operating point based on the ARIES-I design, except for 75% of the α-particle power diverted to fast deuterium ions at 70 KeV. Impurities and external heating are included (Q=40). Note, in this example, for comparison, 75% of the α-particle energy is diverted from 100% of the α particles. In other words, here it is imagined that waves cool all α particles from 3.5 MeV to 875 KeV, rather than, as imagined in all the other examples in this paper, that waves extract 100% of the α-particle energy from 75% of the particles.

$\beta_0(10^{14}\text{KeV/cm}^3)$	514.0
$T_i(\text{KeV})$	55.0
$T_e(\text{KeV})$	55.0
η	0.21
η_w	0
ϕ	0
ρ_i	0.88
ρ_e	0.67
$\nu(\text{sec})$	0.80
$\tau_i(\text{sec})$	6.40
$\tau_e(\text{sec})$	2.54
$n_i(10^{14}/\text{cm}^3)$	1.96
$n_e(10^{14}/\text{cm}^3)$	2.94
$P_f(\text{Watts/cm}^3)$	1.93
$\beta_{\alpha H}/\beta_0$	0.02
β_{pH}/β_0	0.20
β_i/β_0	0.31
β_e/β_0	0.47
$\tau_\alpha(\text{sec})$	0.38
$\tau_p(\text{sec})$	1.05

Table 8: Operating point based on the ARIES-III design.

$\beta_0(10^{14}\text{KeV/cm}^3)$	514.0
$T_i(\text{KeV})$	55.0
$T_e(\text{KeV})$	40.3
η	0.64
η_w	0.75
ϕ	0
χ_α	0.30
ρ_i	0.94
ρ_e	0.62
$\nu(\text{sec})$	1.66
$\tau_i(\text{sec})$	6.81
$\tau_e(\text{sec})$	0.97
$n_i(10^{14}/\text{cm}^3)$	2.57
$n_e(10^{14}/\text{cm}^3)$	3.86
$P_f(\text{Watts/cm}^3)$	4.33
$\beta_{\alpha H}/\beta_0$	0.01
β_{pH}/β_0	0.06
β_{fi}/β_0	0.07
β_i/β_0	0.41
β_e/β_0	0.45
$\tau_\alpha(\text{sec})$	0.23
$\tau_p(\text{sec})$	0.51

Table 9: Operating point based on the ARIES-III design, except for 75% of the fusion product power diverted to 350 KeV deuterium ions.

$\beta_0(10^{14}\text{KeV/cm}^3)$	514.0
$T_i(\text{KeV})$	55.0
$T_e(\text{KeV})$	40.7
η	0.79
η_w	0.75
ϕ	0
χ_α	0
ρ_i	0.95
ρ_e	0.68
$\nu(\text{sec})$	1.78
$\tau_i(\text{sec})$	6.48
$\tau_e(\text{sec})$	1.21
$n_i(10^{14}/\text{cm}^3)$	2.80
$n_e(10^{14}/\text{cm}^3)$	4.20
$P_f(\text{Watts/cm}^3)$	3.95
$\beta_{\alpha H}/\beta_0$	0.01
β_{pH}/β_0	0.04
β_{fi}/β_0	0.00
β_i/β_0	0.45
β_e/β_0	0.50
$\tau_\alpha(\text{sec})$	0.21
$\tau_p(\text{sec})$	0.48

Table 10: Operating point based on the ARIES-III design, except for 75% of the fusion product power diverted to bulk fuel ions.

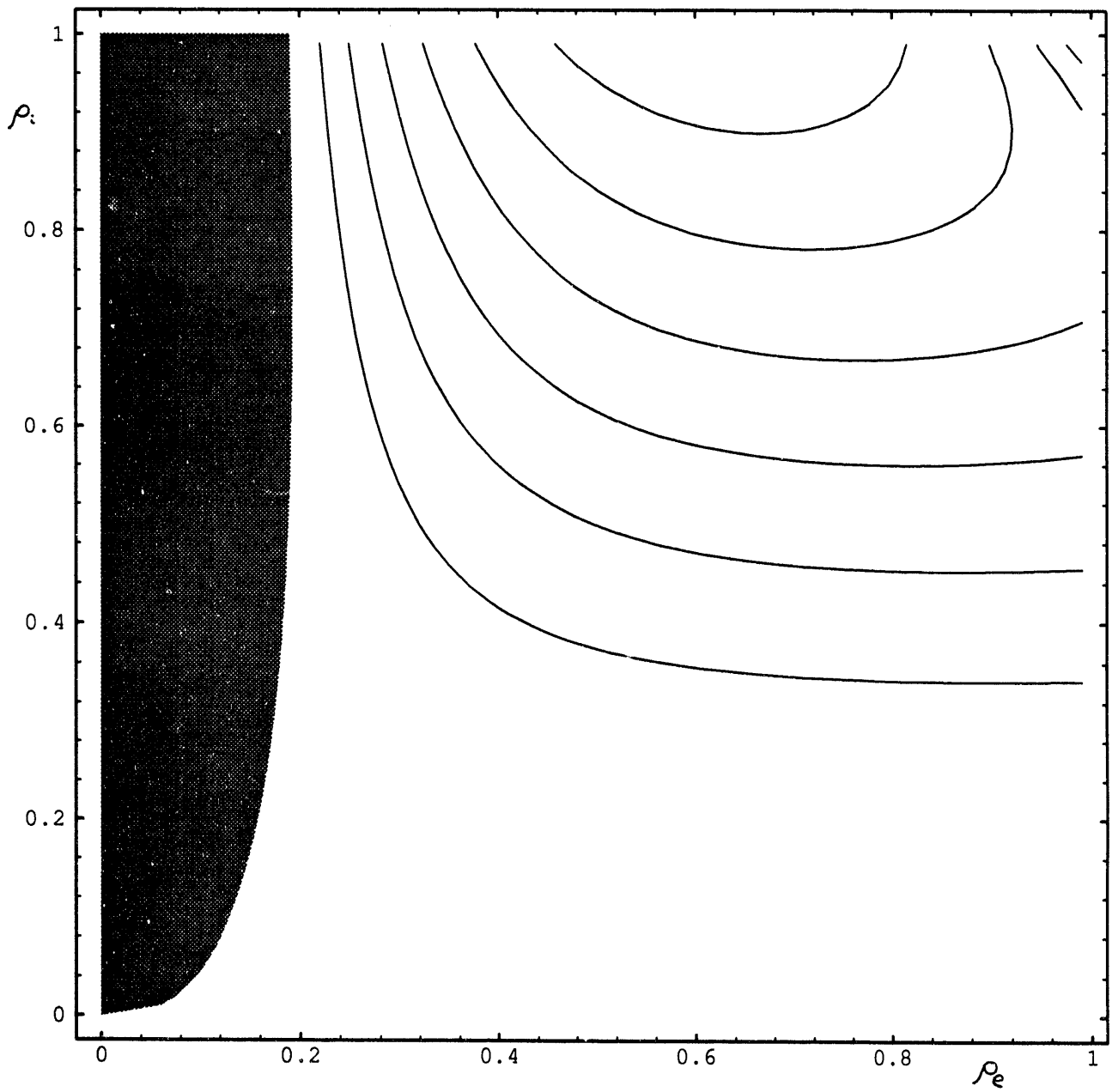

Figure 1-a: Contours of P_f versus ρ_e and ρ_i, with β_0=91, η=0.28, $\nu\tau_\alpha$=0.30. Contours from bottom to top are P_f (Watts/cm^3)=2, 3, 4, 5, 6, 7.

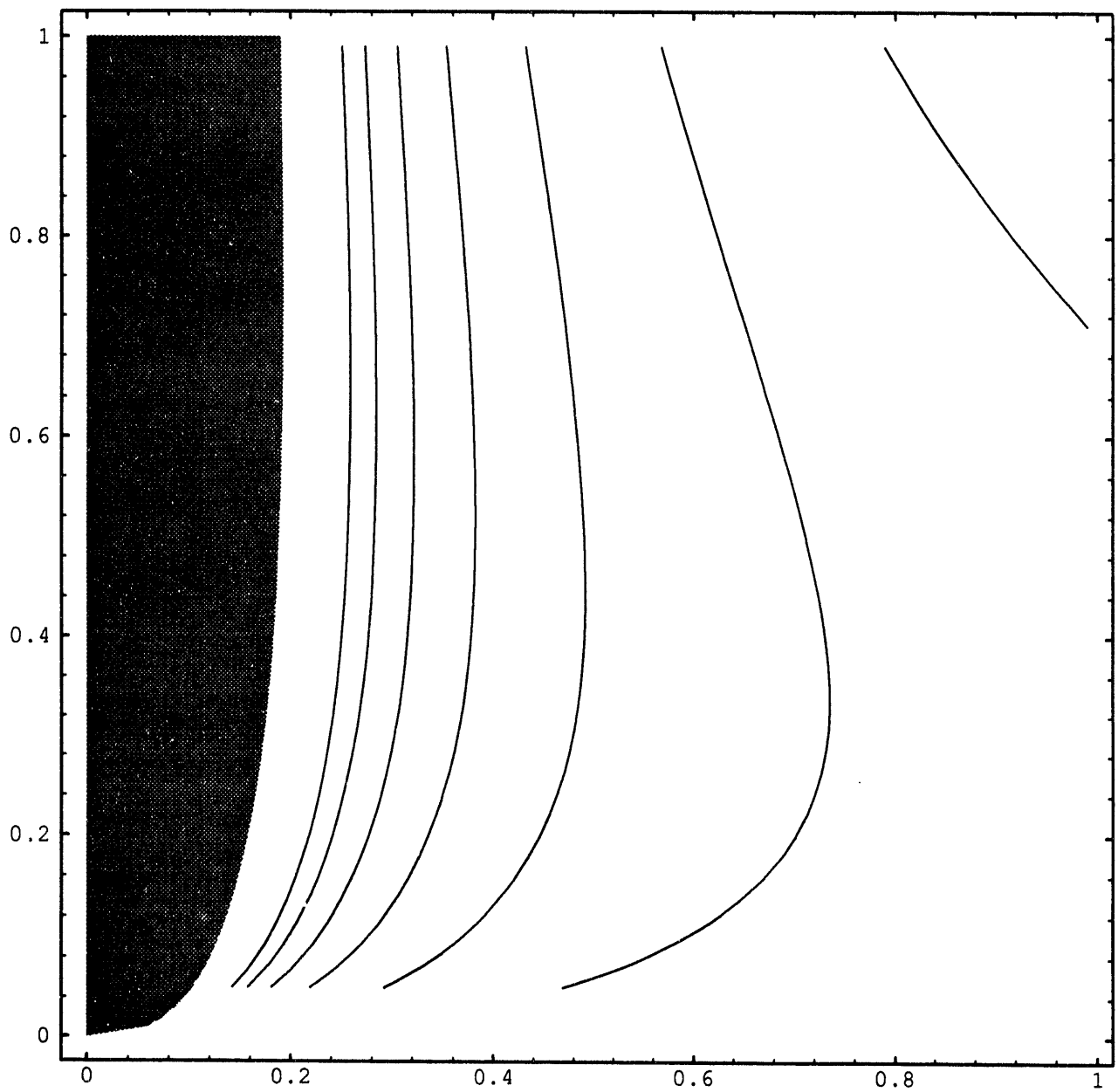

Figure 1-b: Contours of T_i versus ρ_e and ρ_i, with β_0=91, η=0.28, $\nu\tau_\alpha$=0.30. Contours from left to right are T_i (KeV)=40, 35, 30, 25, 20, 15, 10.

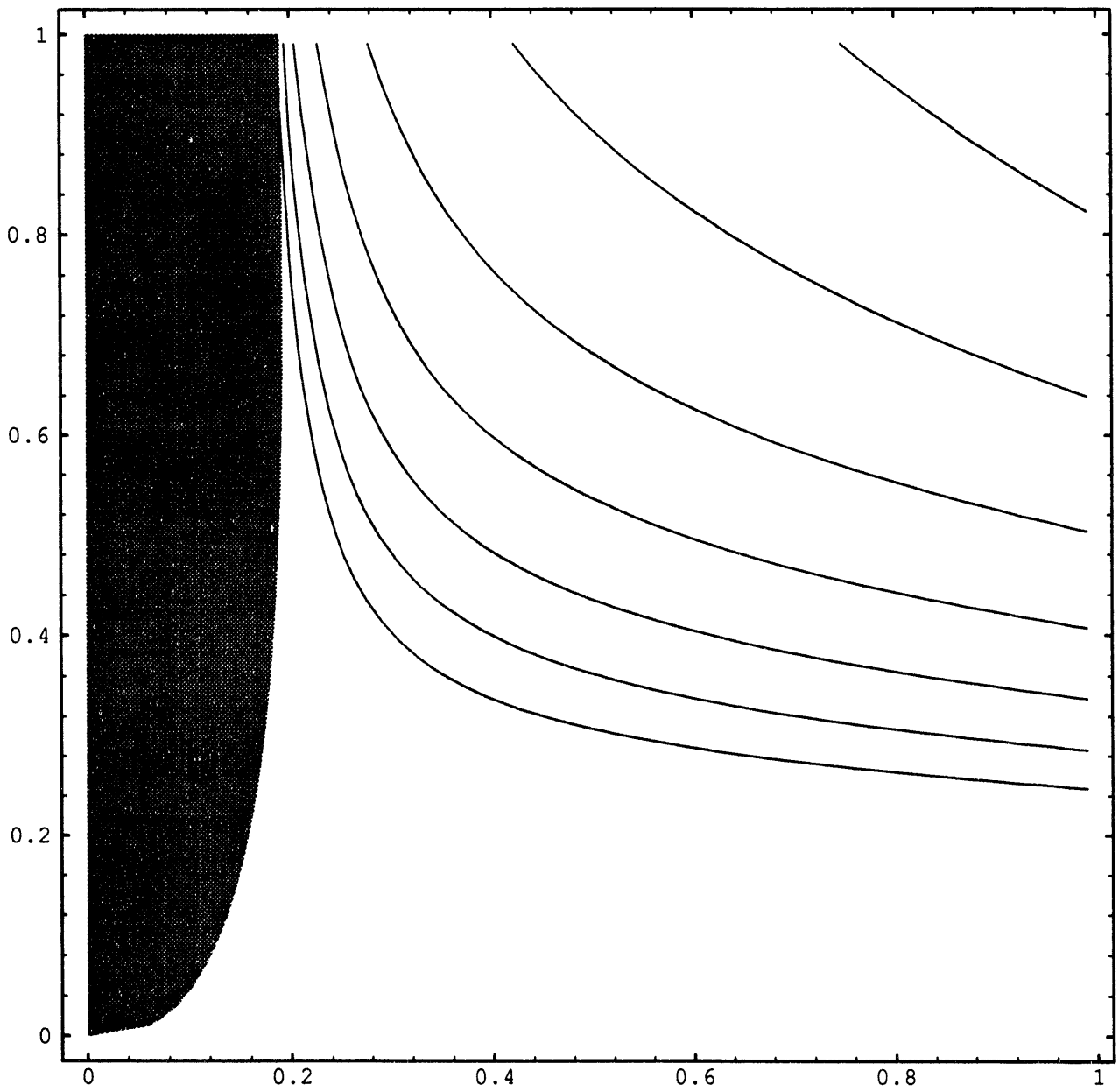

Figure 1-c: Contours of T_e versus ρ_e and ρ_i, with β_0=91, η=0.28, $\nu\tau_\alpha$=0.30. Contours from left to right are T_e (KeV)=40, 35, 30, 25, 20, 15, 10.

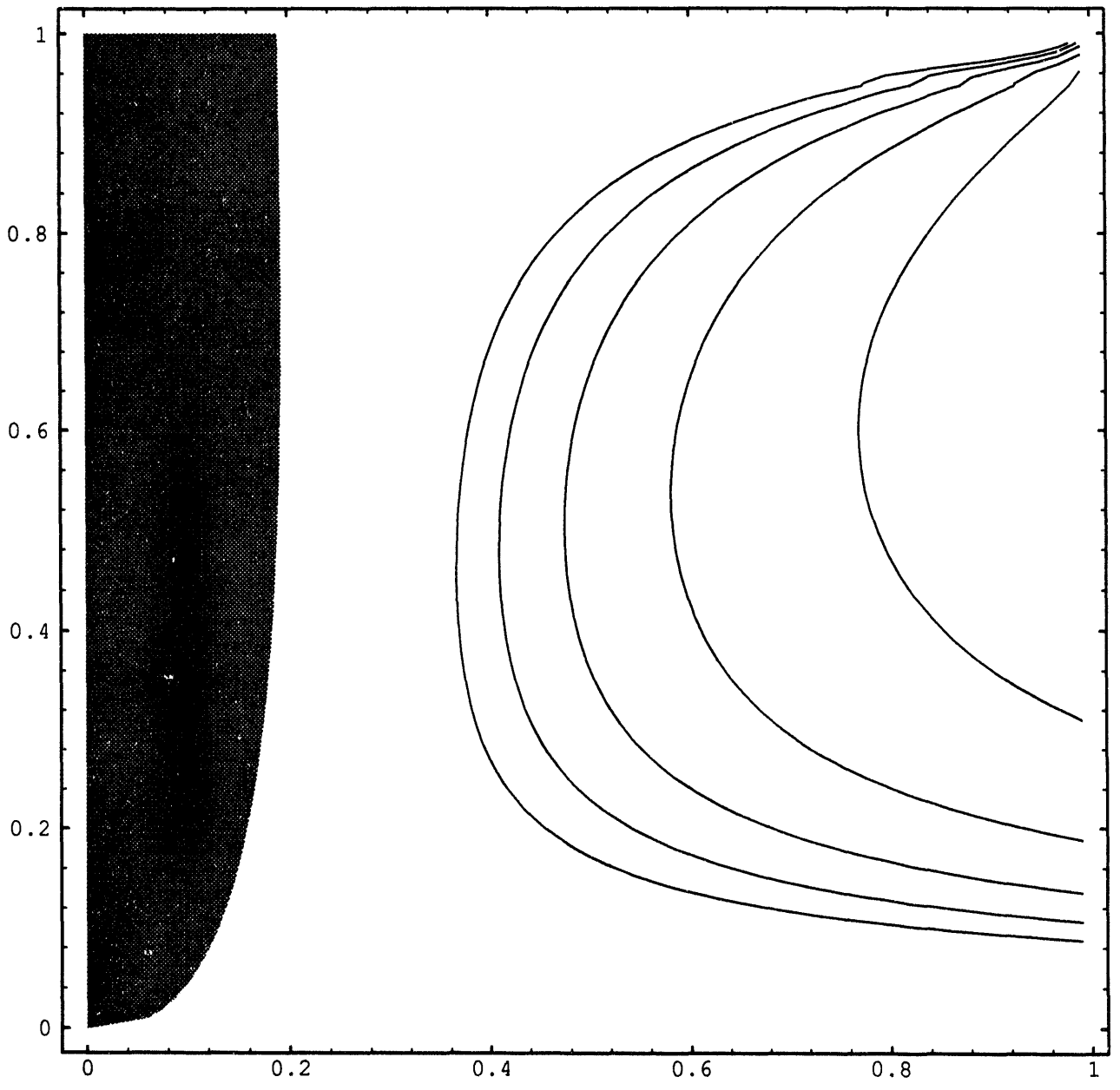

Figure 1-d: Contours of τ_i versus ρ_e and ρ_i, with β_0=91, η=0.28, $\nu\tau_\alpha$=0.30. Contours from left to right are τ_i (sec)=3.0, 2.5, 2.0, 1.5, 1.0.

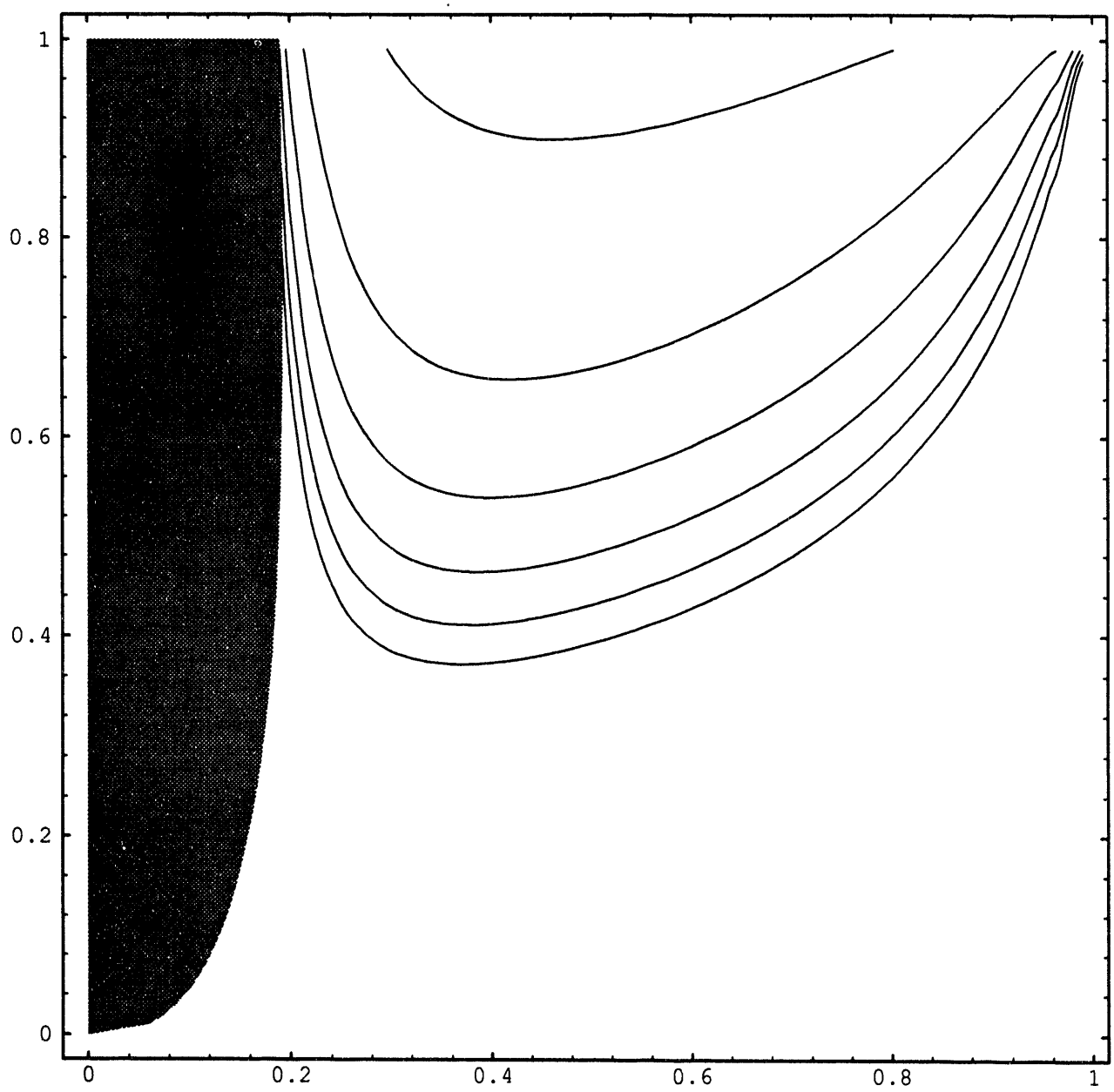

Figure 1-e: Contours of τ_e versus ρ_e and ρ_i, with β_0=91, η=0.28, $\nu\tau_\alpha$=0.30. Contours from bottom to top are τ_e (sec)=3.0, 2.5, 2.0, 1.5, 1.0, 0.5.

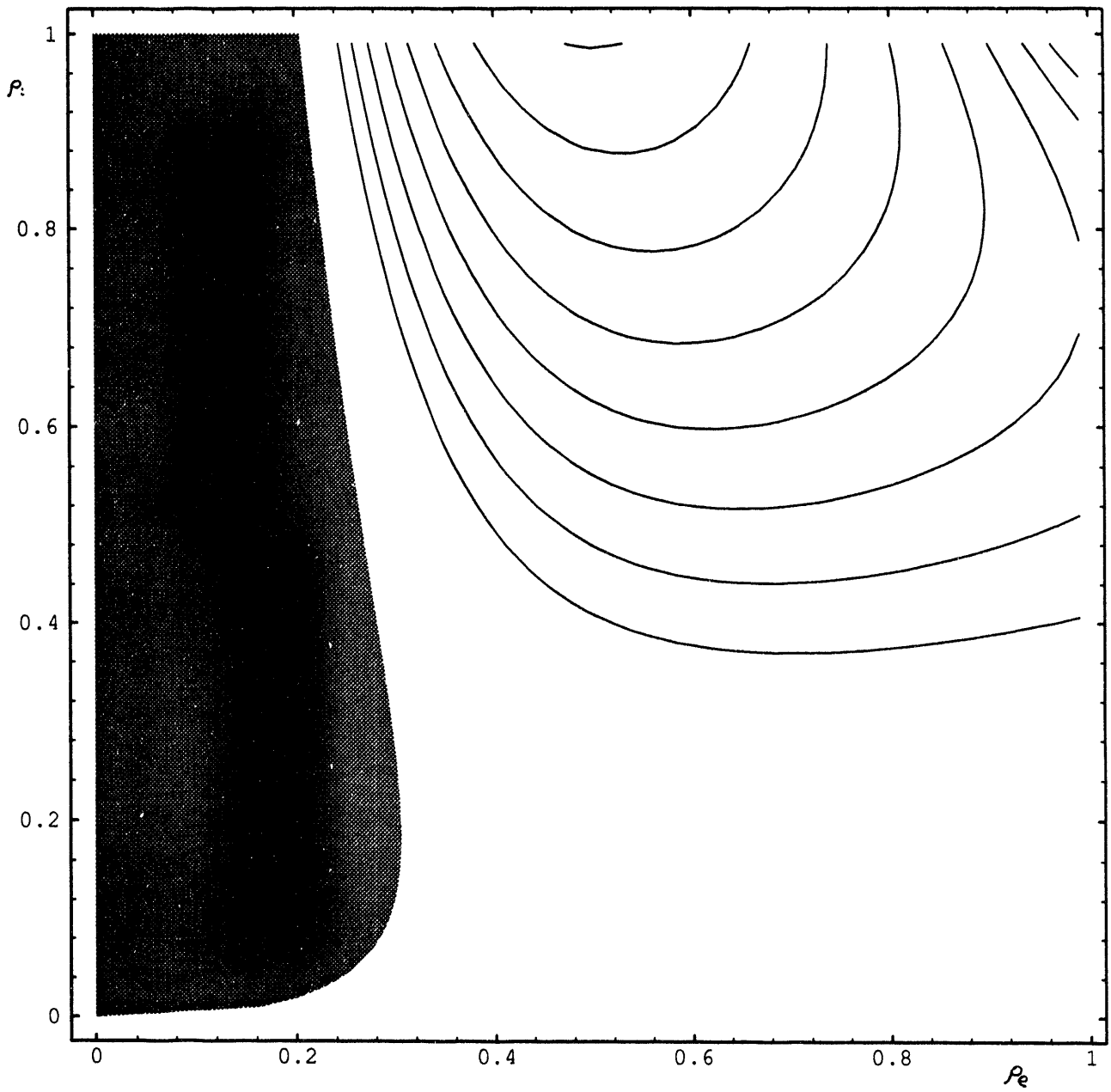

Figure 2-a: Contours of P_f versus ρ_e and ρ_i, with β_0=91, η=0.69, η_w=0.75, χ_α=0.16, $\nu\tau_\alpha$=0.32. Diverted α-particle power is applied to deuterium ions at 70 KeV. Contours from bottom to top are P_f (Watts/cm^3)=5, 6, 7, 8, 9, 10, 11, 12.

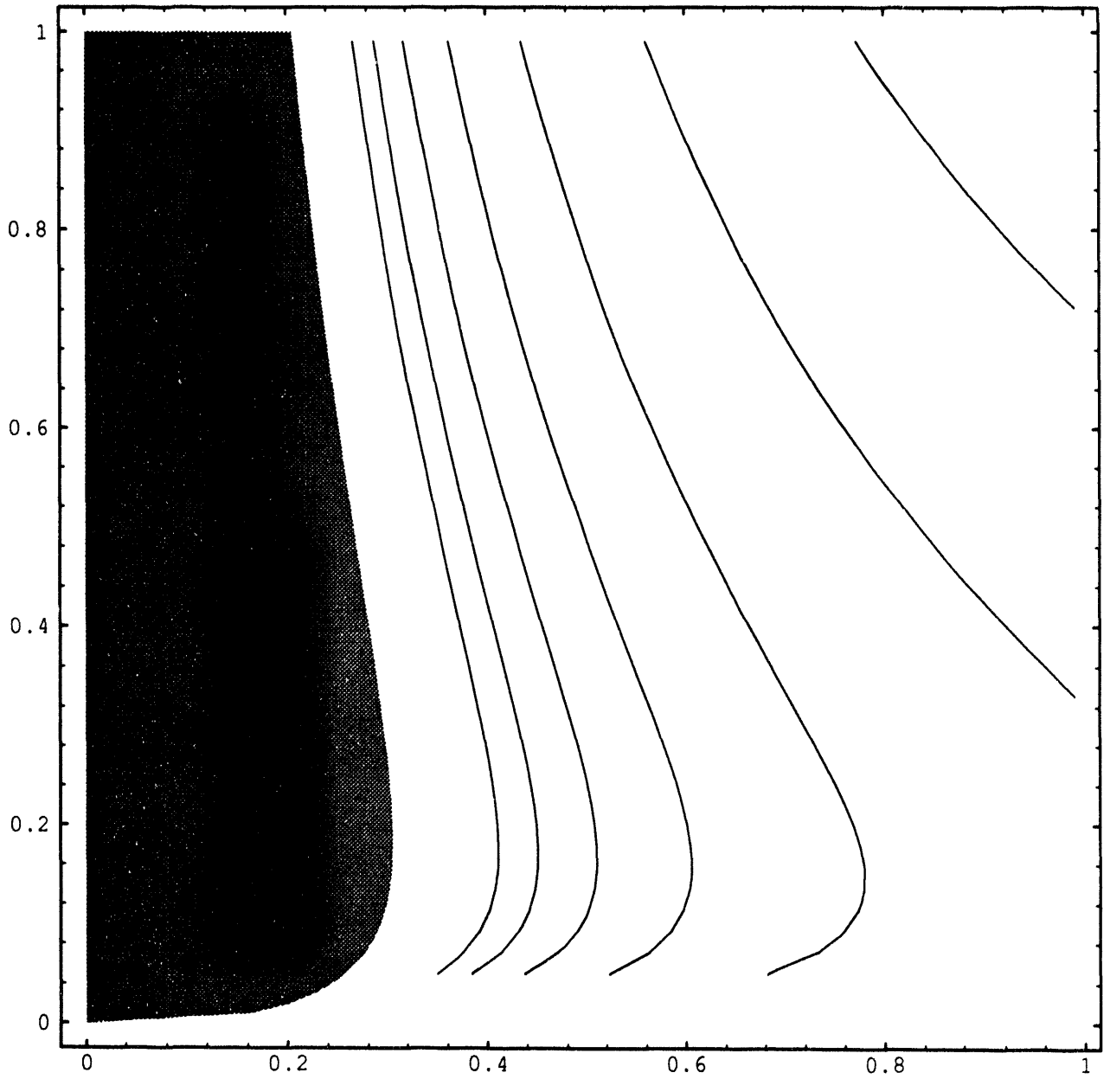

Figure 2-b: Contours of T_i versus ρ_e and ρ_i, with β_0=91, η=0.69, η_w=0.75, χ_α=0.16, $\nu\tau_\alpha$=0.32. Diverted α-particle power is applied to deuterium ions at 70 KeV. Contours from left to right are T_i (KeV)=40, 35, 30, 25, 20, 15, 10.

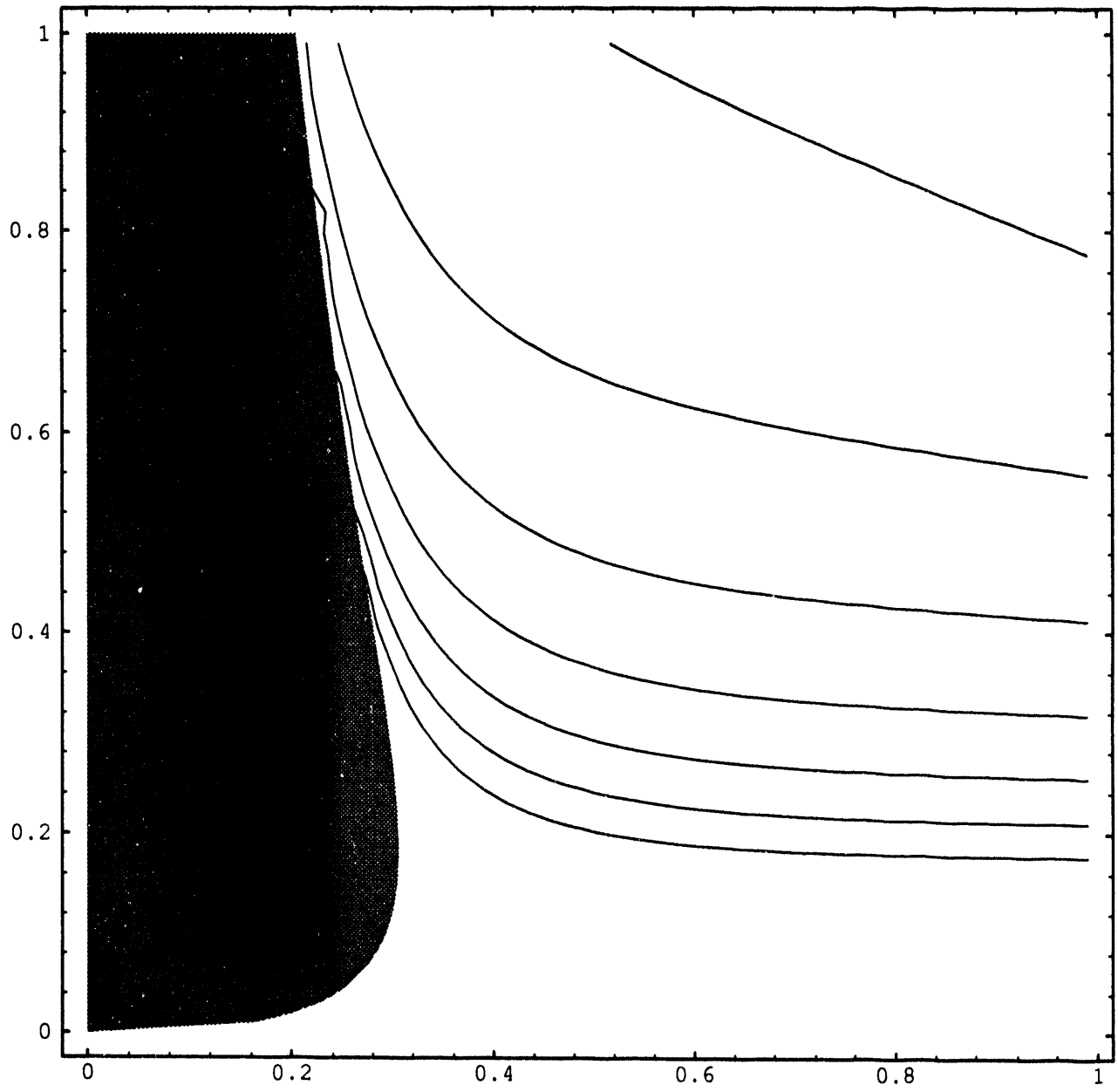

Figure 2-c: Contours of T_e versus ρ_e and ρ_i, with β_0=91, η=0.69, η_w=0.75, χ_α=0.16, $\nu\tau_\alpha$=0.32. Diverted α-particle power is applied to deuterium ions at 70 KeV. Contours from left to right are T_e (KeV)=40, 35, 30, 25, 20, 15, 10.

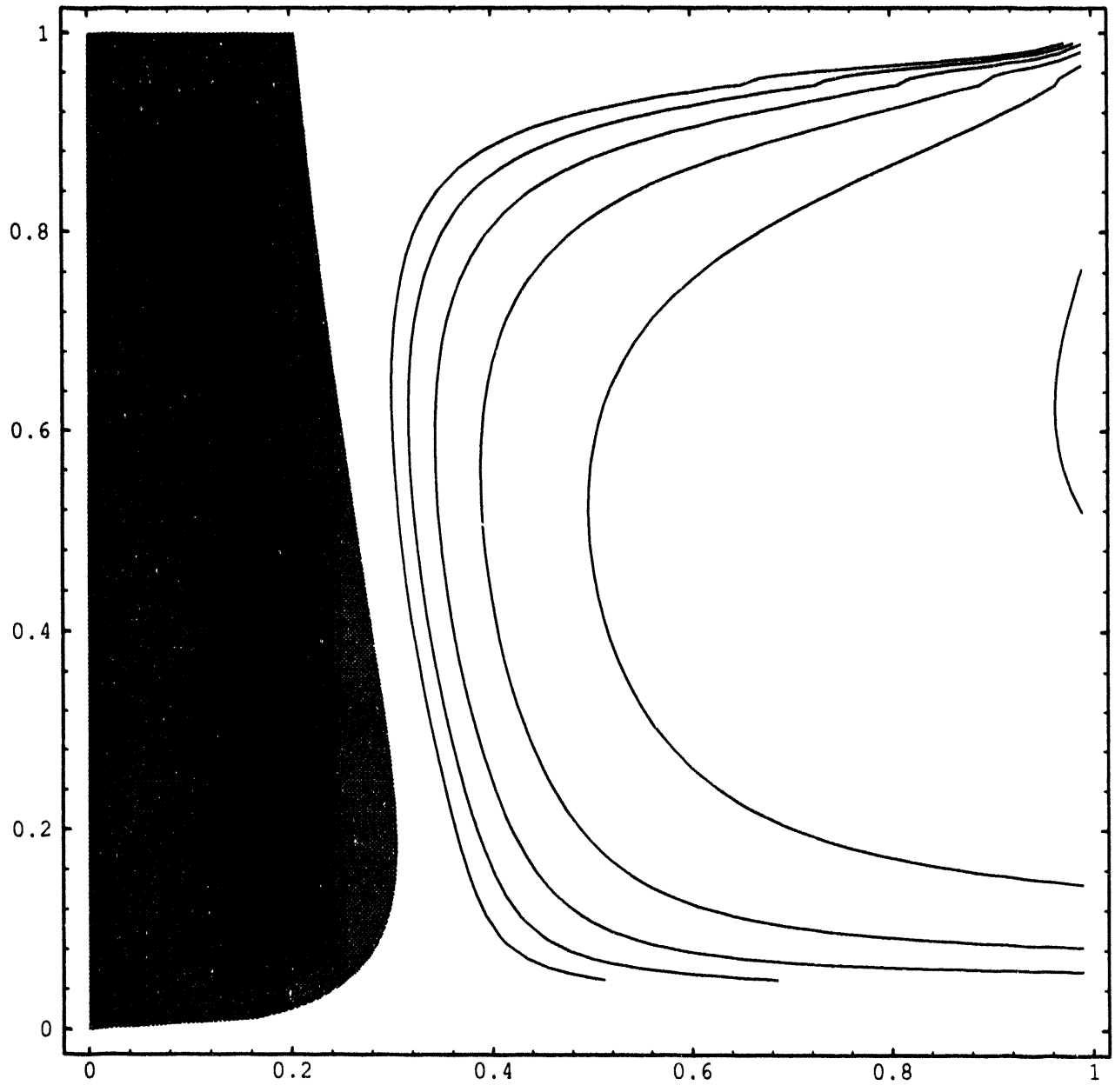

Figure 2-d: Contours of τ_i versus ρ_e and ρ_i, with β_0=91, η=0.69, η_w=0.75, χ_α=0.16, $\nu\tau_\alpha$=0.32. Diverted α-particle power is applied to deuterium ions at 70 KeV. Contours from left to right are τ_i (sec)=3.0, 2.5, 2.0, 1.5, 1.0, 0.5.

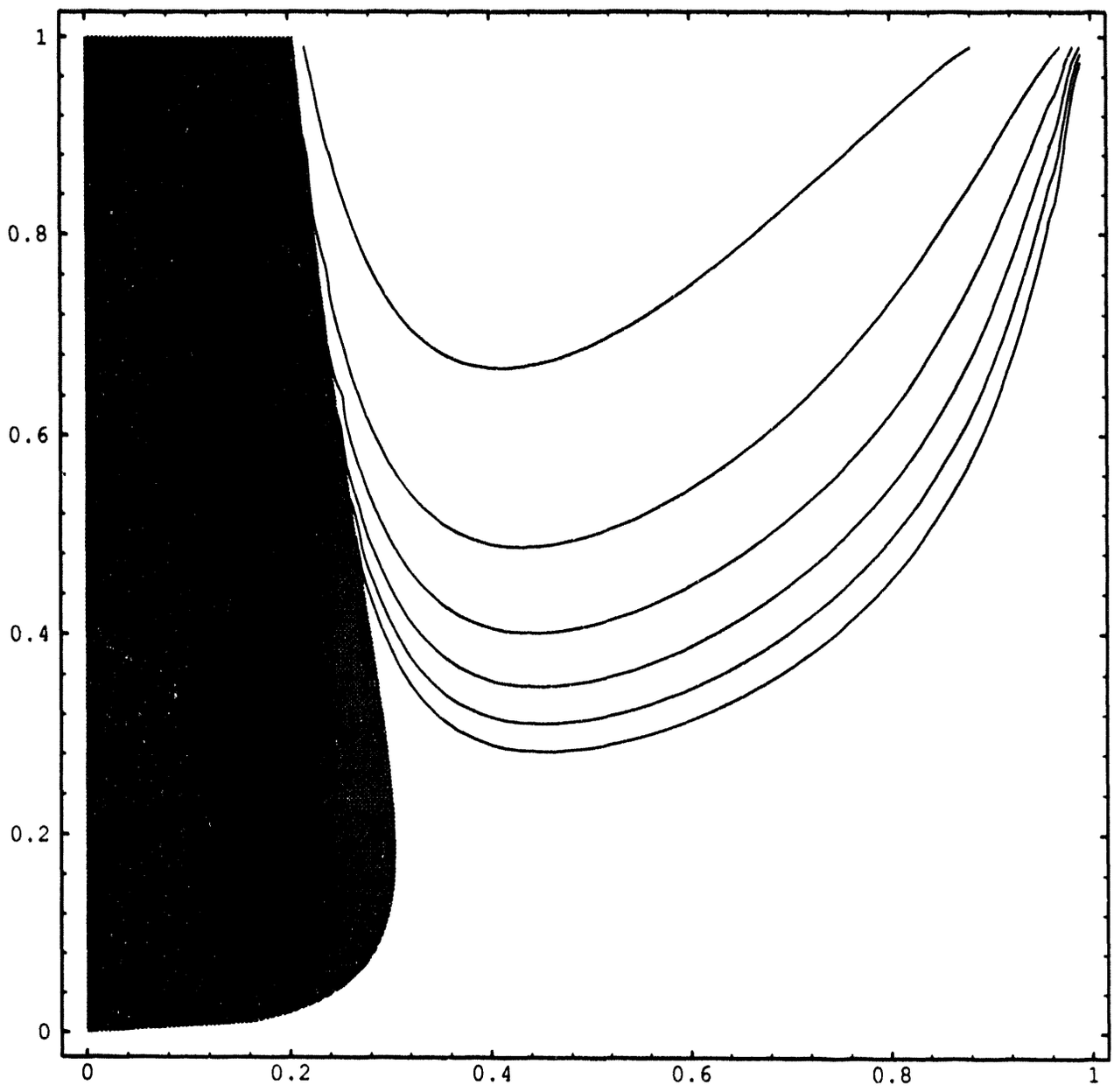

Figure 2-e: Contours of τ_e versus ρ_e and ρ_i, with β_0=91, η=0.69, η_w=0.75, χ_α=0.16, $\nu\tau_\alpha$=0.32. Diverted α-particle power is applied to deuterium ions at 70 KeV. Contours from bottom to top are τ_e (sec)=3.0, 2.5, 2.0, 1.5, 1.0, 0.5.

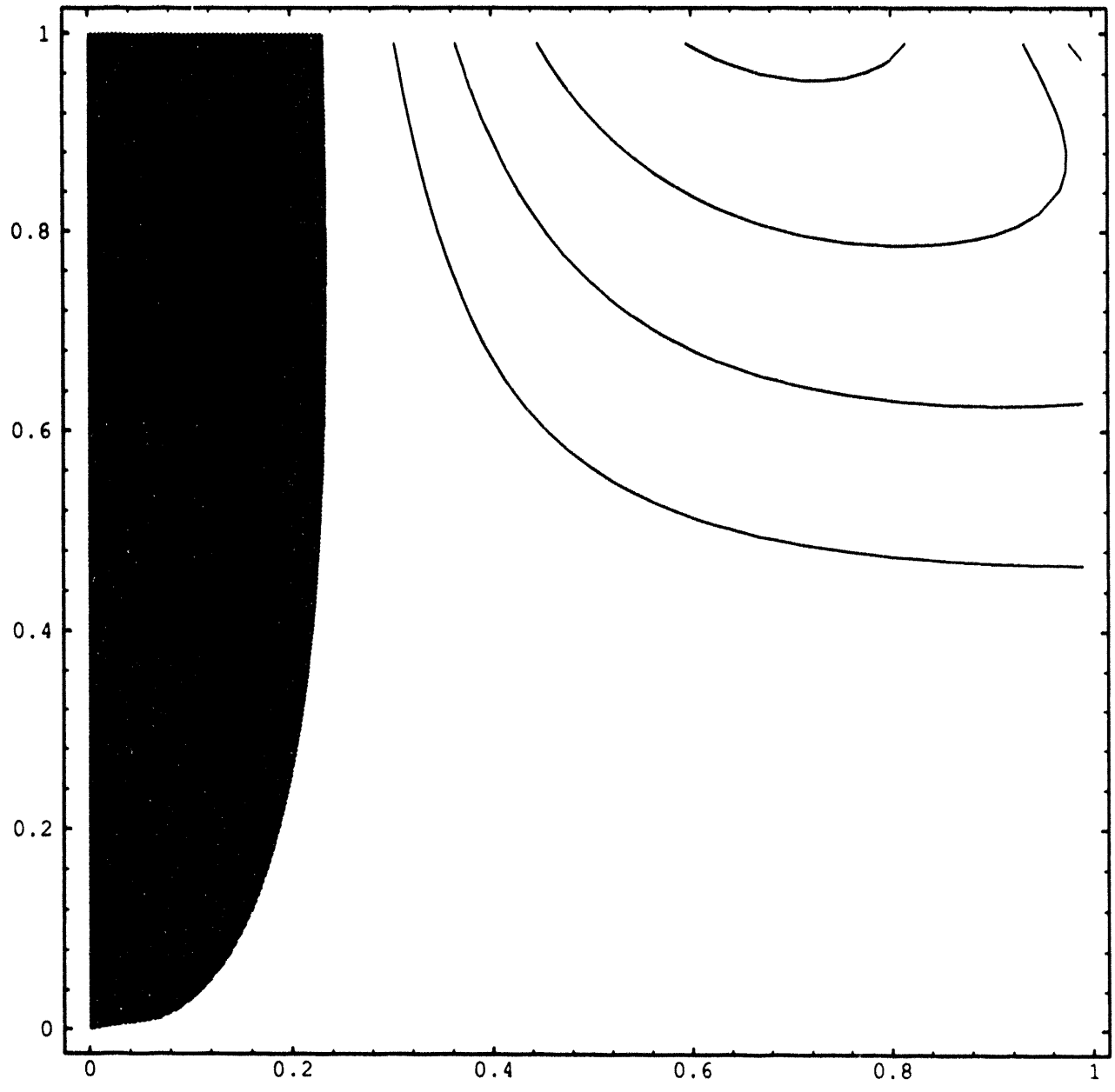

Figure 3-a: Contours of P_f versus ρ_e and ρ_i, with β_0=91, η=0.23, $\nu\tau_\alpha$=0.31. External heating with ϕ=0.25 is applied to the electrons. Impurities with Z_{eff}=1.65 are present. Contours from bottom to top are P_f (Watts/cm^3)=2, 3, 4, 5.

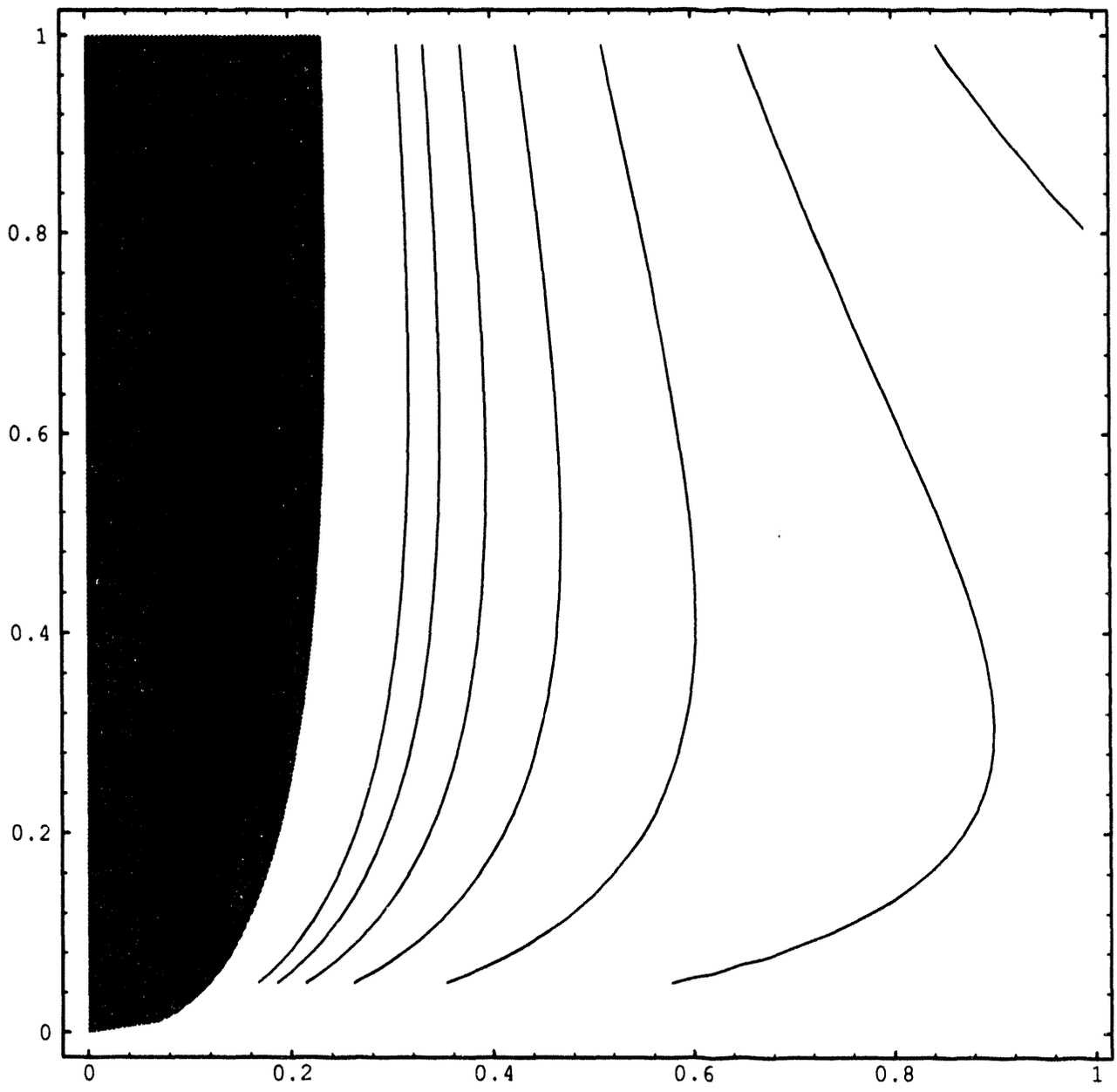

Figure 3-b: Contours of T_i versus ρ_e and ρ_i, with β_0=91, η=0.23, $\nu\tau_\alpha$=0.31. External heating with ϕ=0.25 is applied to the electrons. Impurities with Z_{eff}=1.65 are present. Contours from left to right are T_i (KeV)=40, 35, 30, 25, 20, 15, 10.

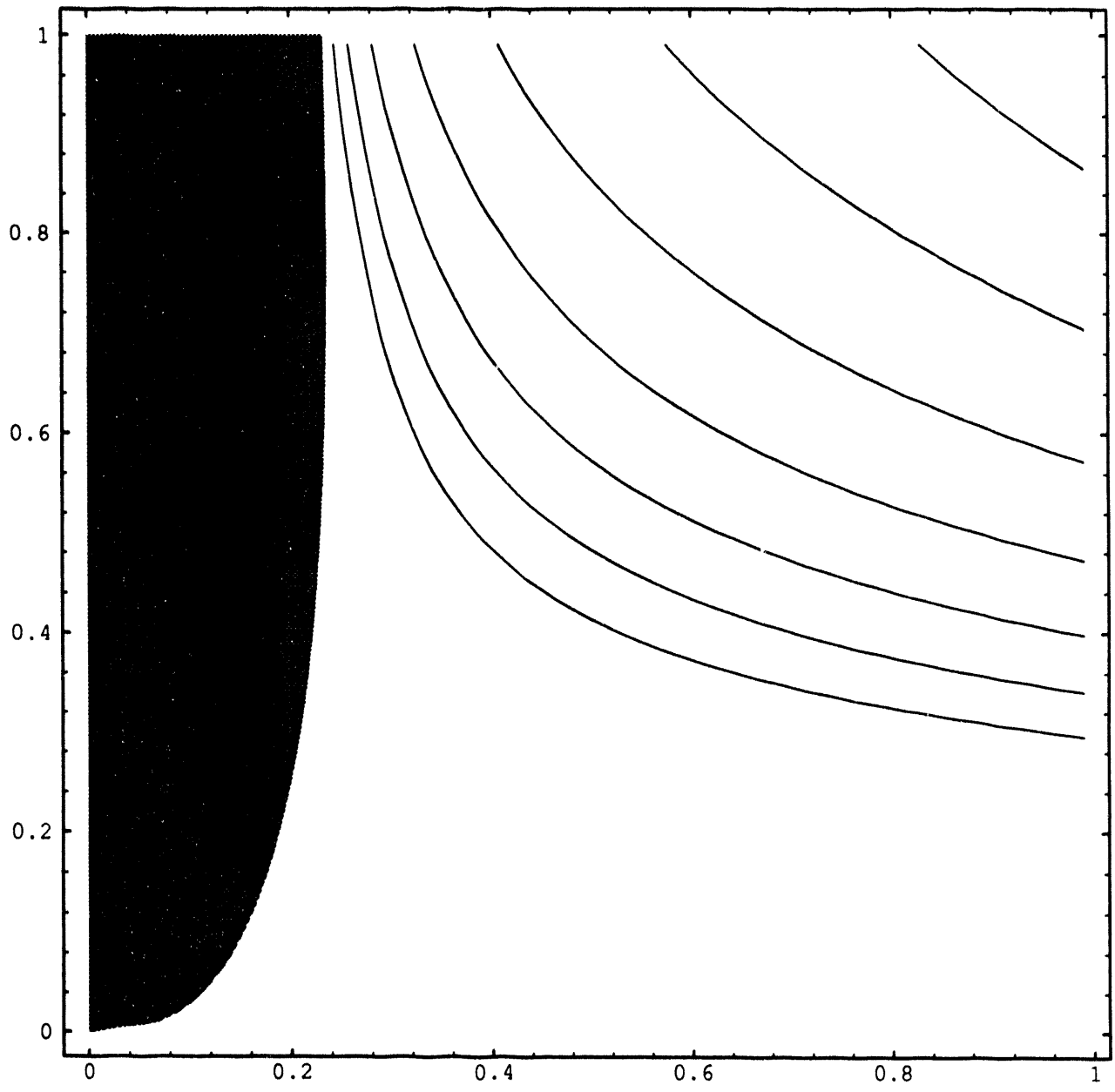

Figure 3-c: Contours of T_e versus ρ_e and ρ_i, with β_0=91, η=0.23, $\nu\tau_\alpha$=0.31. External heating with ϕ=0.25 is applied to the electrons. Impurities with Z_{eff}=1.65 are present. Contours from left to right are T_e (KeV)=40, 35, 30, 25, 20, 15, 10.

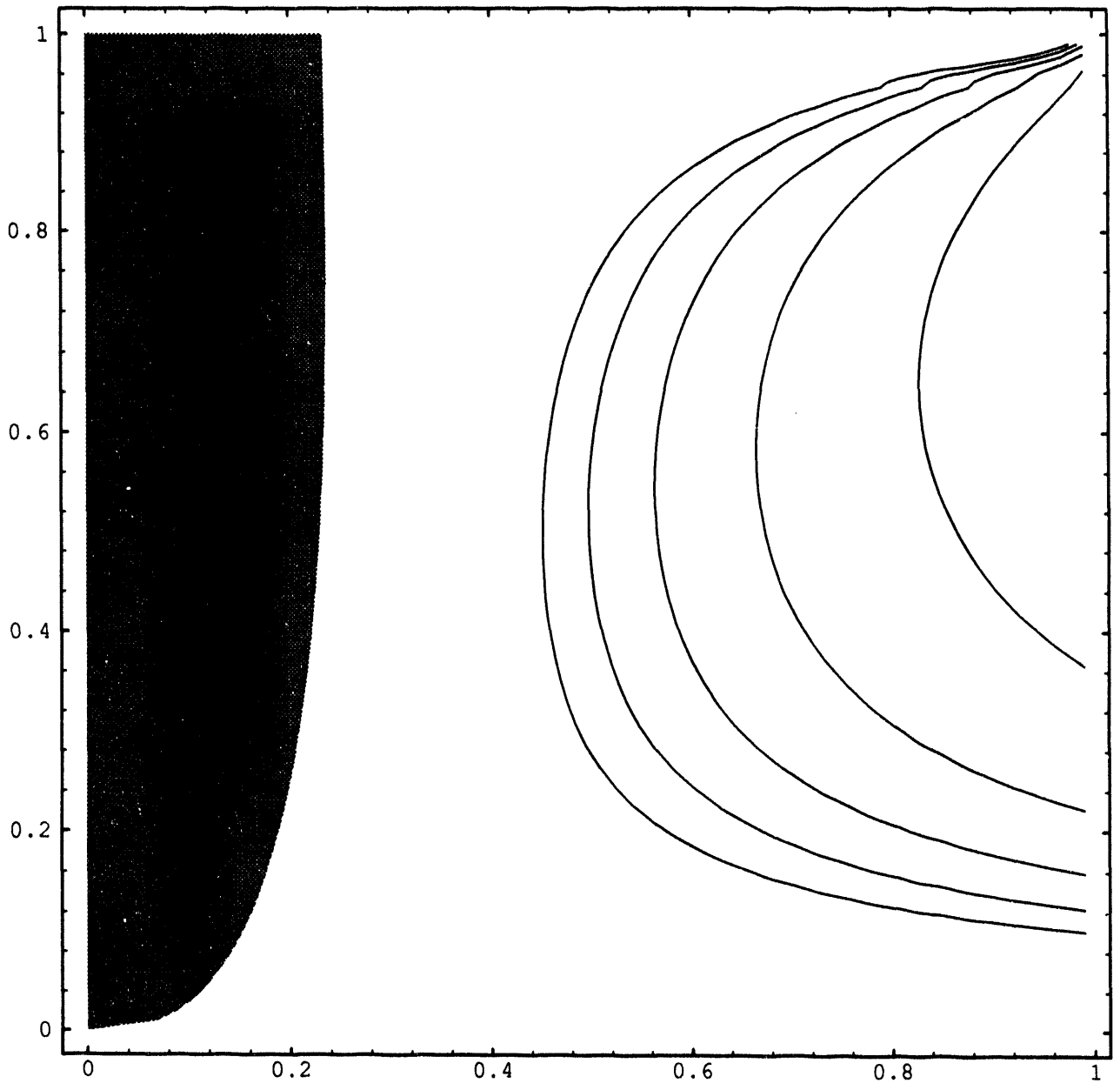

Figure 3-d: Contours of τ_i versus ρ_e and ρ_i, with β_0=91, η=0.23, $\nu\tau_\alpha$=0.31. External heating with ϕ=0.25 is applied to the electrons. Impurities with Z_{eff}=1.65 are present. Contours from left to right are τ_i (sec)=3.0, 2.5, 2.0, 1.5, 1.0.

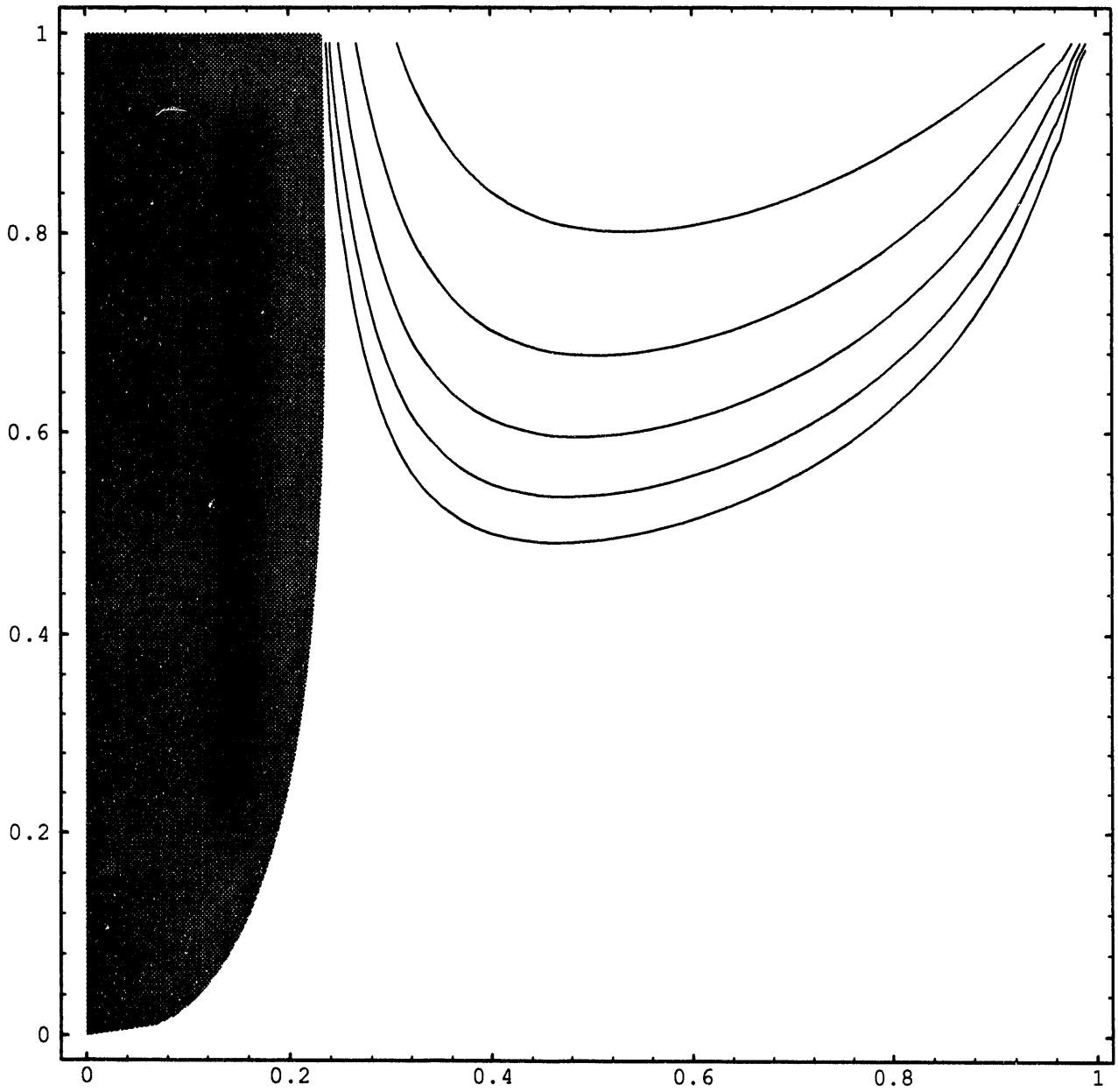

Figure 3-e: Contours of τ_e versus ρ_e and ρ_i, with β_0=91, η=0.23, $\nu\tau_\alpha$=0.31. External heating with ϕ=0.25 is applied to the electrons. Impurities with Z_{eff}=1.65 are present. Contours from bottom to top are τ_e (sec)=3.0, 2.5, 2.0, 1.5, 1.0.

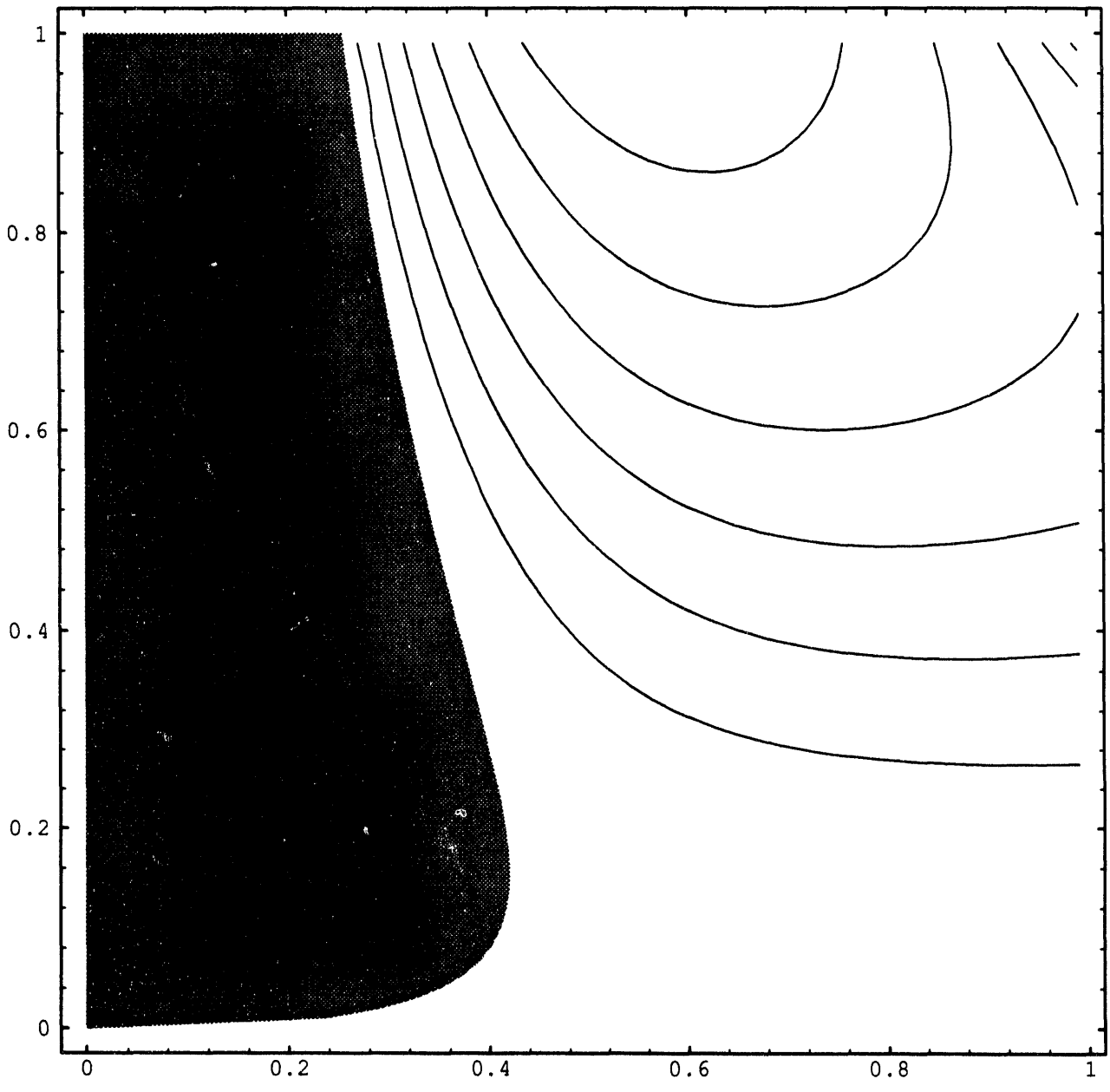

Figure 4-a: Contours of P_f versus ρ_e and ρ_i, with β_0=91, η=0.72, η_w=0.75, χ_α=0.12, $\nu\tau_\alpha$=0.33. Diverted α-particle power and external heating with ϕ=0.25 are applied to deuterium ions at 70 KeV. Impurities with Z_{eff}=1.65 are present. Contours from bottom to top are P_f (Watts/cm^3)=2, 3, 4, 5, 6, 7.

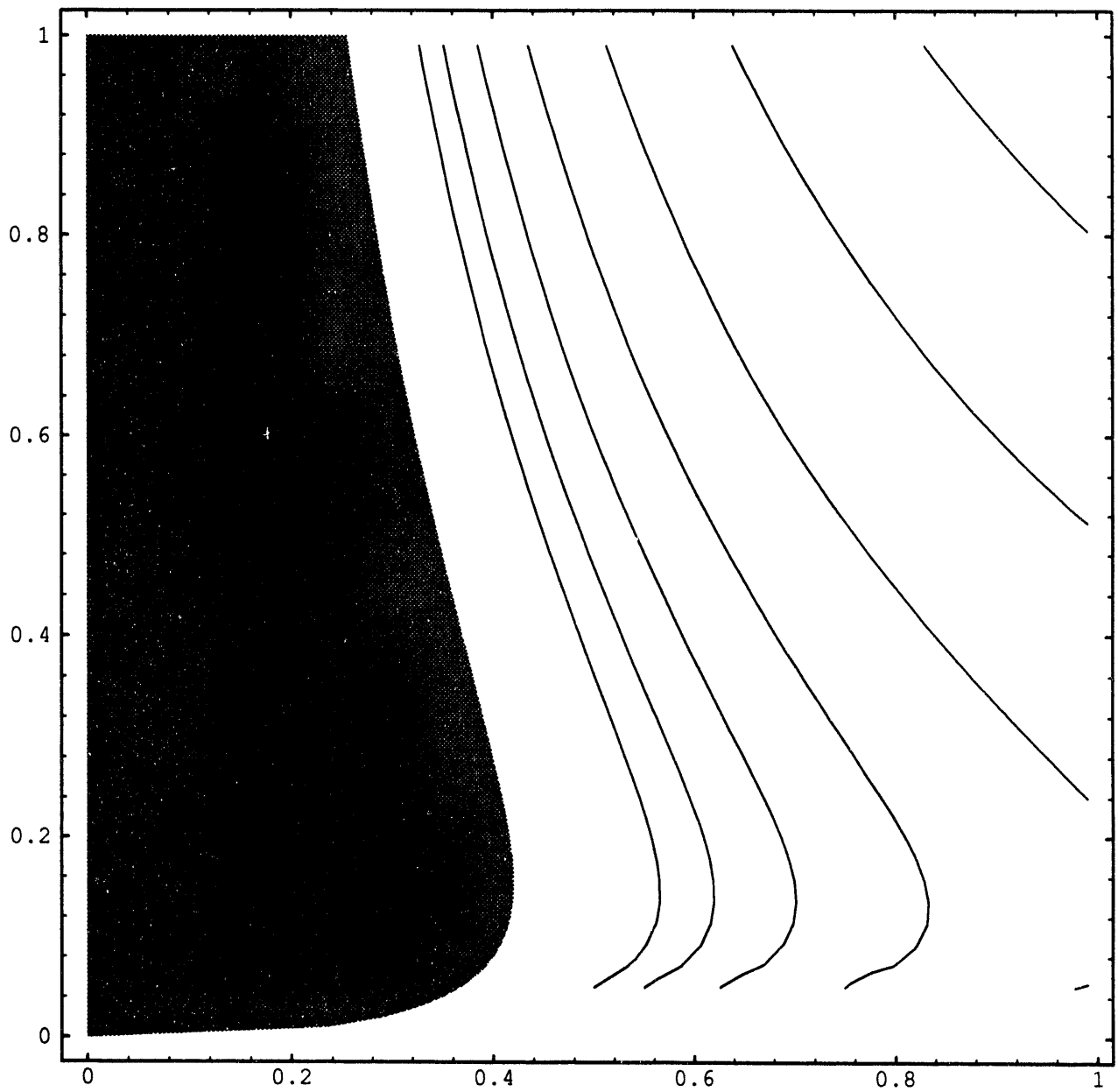

Figure 4-b: Contours of T_i versus ρ_e and ρ_i, with β_0=91, η=0.72, η_w=0.75, χ_α=0.12, $\nu\tau_\alpha$=0.33. Diverted α-particle power and external heating with ϕ=0.25 are applied to deuterium ions at 70 KeV. Impurities with Z_{eff}=1.65 are present. Contours from left to right are T_i (KeV)=40, 35, 30, 25, 20, 15, 10.

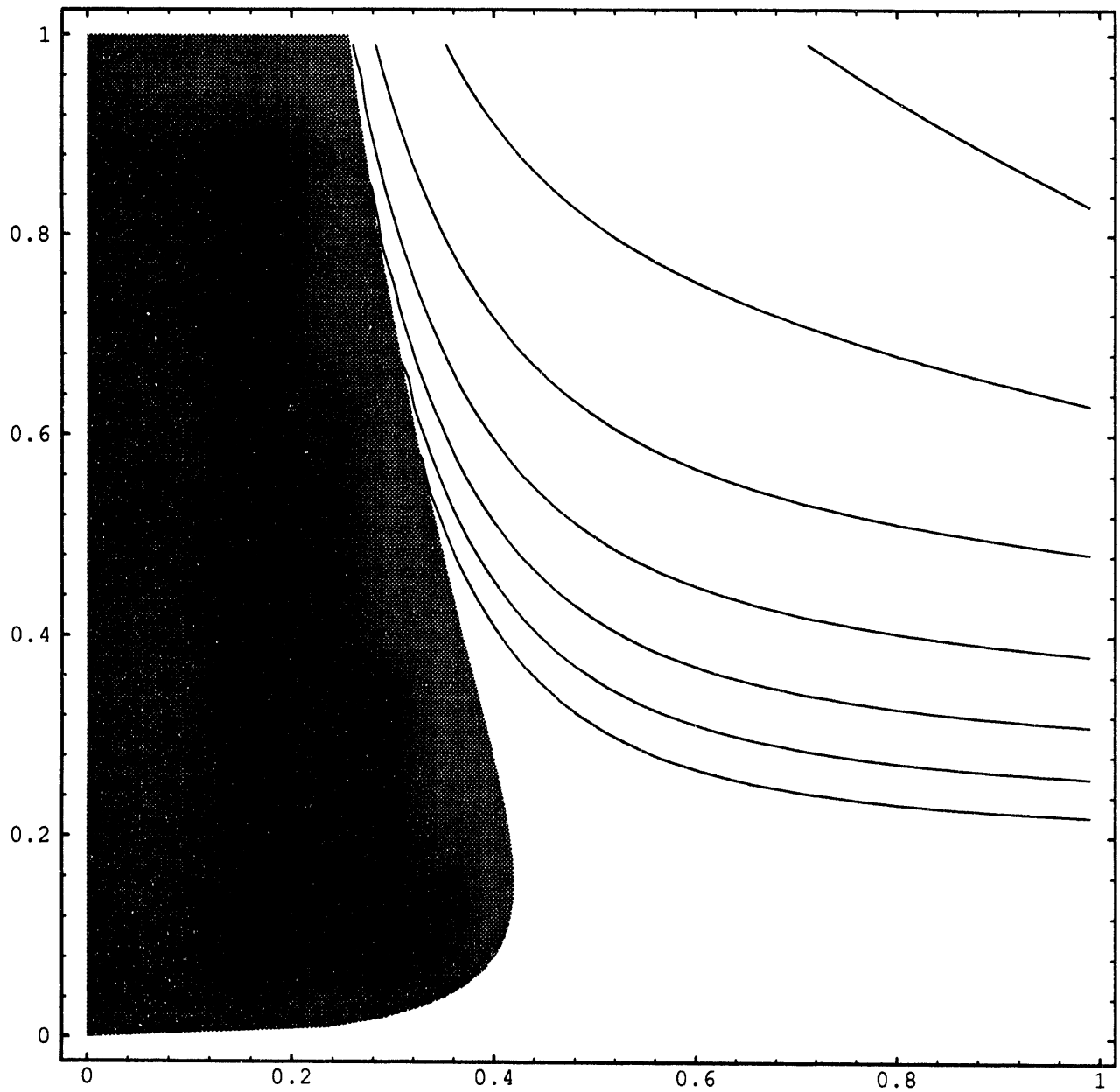

Figure 4-c: Contours of T_e versus ρ_e and ρ_i, with β_0=91, η=0.72, η_w=0.75, χ_α=0.12, $\nu\tau_\alpha$=0.33. Diverted α-particle power and external heating with ϕ=0.25 are applied to deuterium ions at 70 KeV. Impurities with Z_{eff}=1.65 are present. Contours from left to right are T_e (KeV)=40, 35, 30, 25, 20, 15, 10.

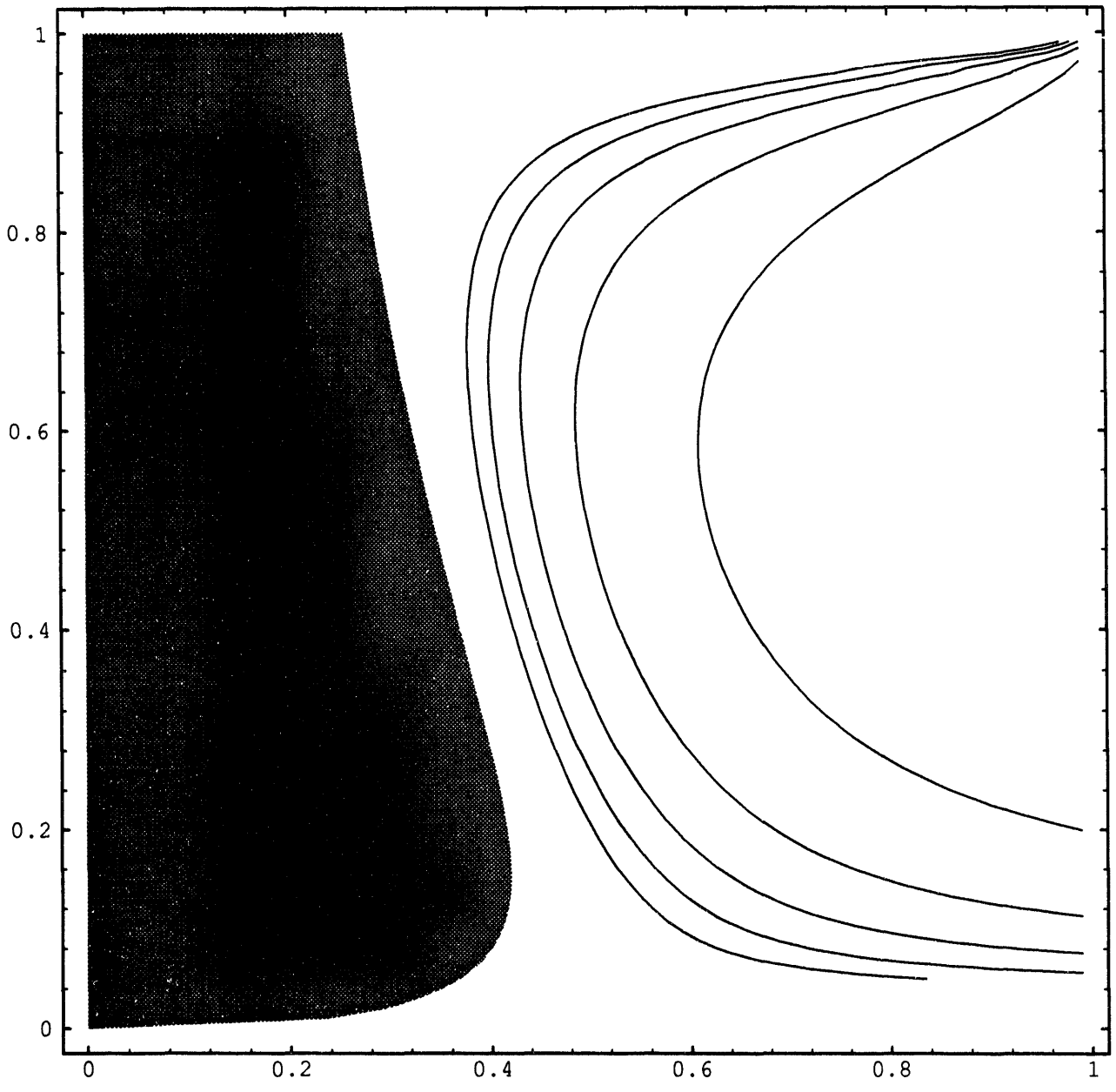

Figure 4-d: Contours of τ_i versus ρ_e and ρ_i, with β_0=91, η=0.72, η_w=0.75, χ_α=0.12, $\nu\tau_\alpha$=0.33. Diverted α-particle power and external heating with ϕ=0.25 are applied to deuterium ions at 70 KeV. Impurities with Z_{eff}=1.65 are present. Contours from left to right are τ_i (sec)=3.0, 2.5, 2.0, 1.5, 1.0.

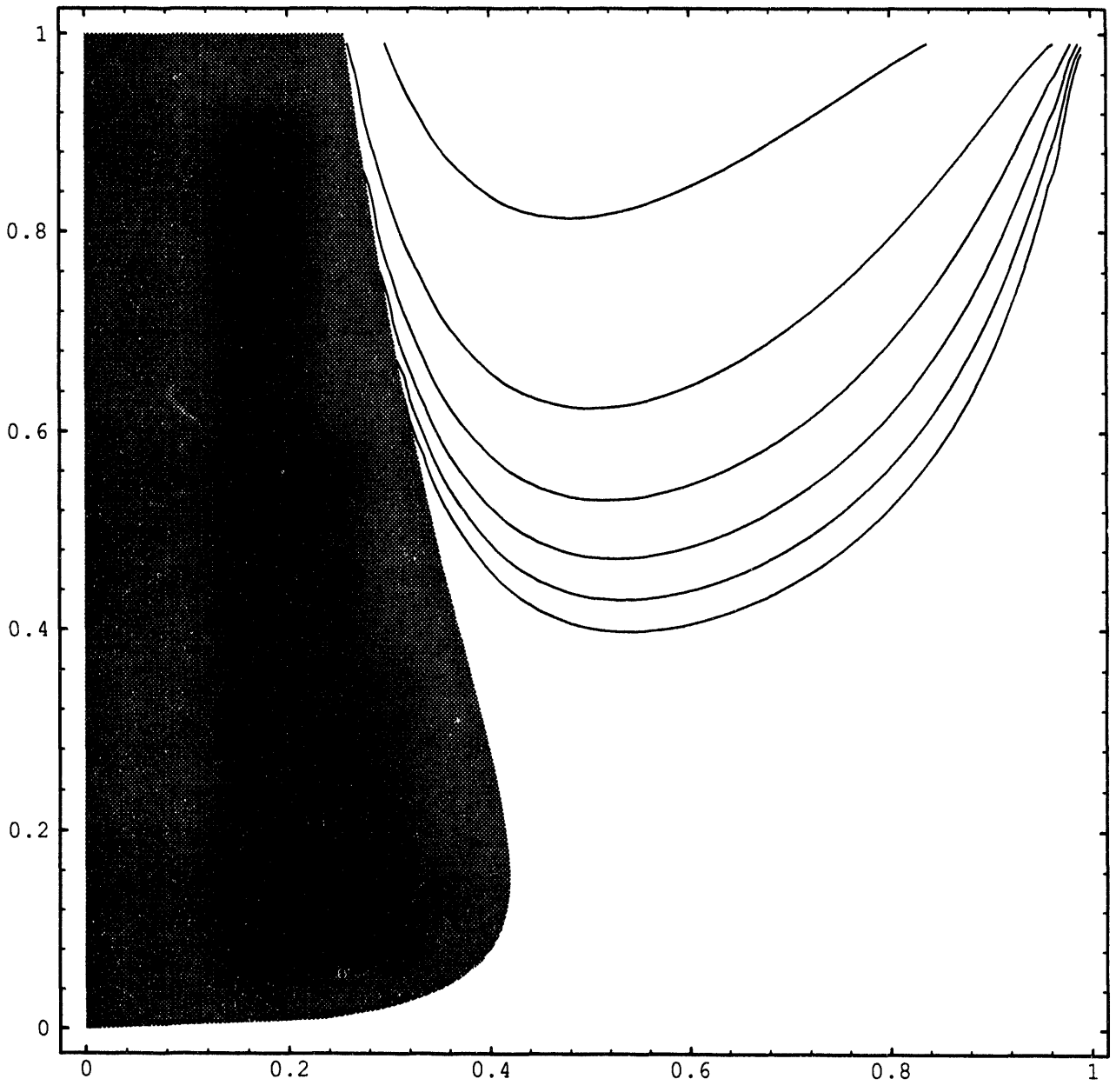

Figure 4-e: Contours of τ_e versus ρ_e and ρ_i, with β_0=91, η=0.72, η_w=0.75, χ_α=0.12, $\nu\tau_\alpha$=0.33. Diverted α-particle power and external heating with ϕ=0.25 are applied to deuterium ions at 70 KeV. Impurities with Z_{eff}=1.65 are present. Contours from bottom to top are τ_e (sec)=3.0, 2.5, 2.0, 1.5, 1.0, 0.5.

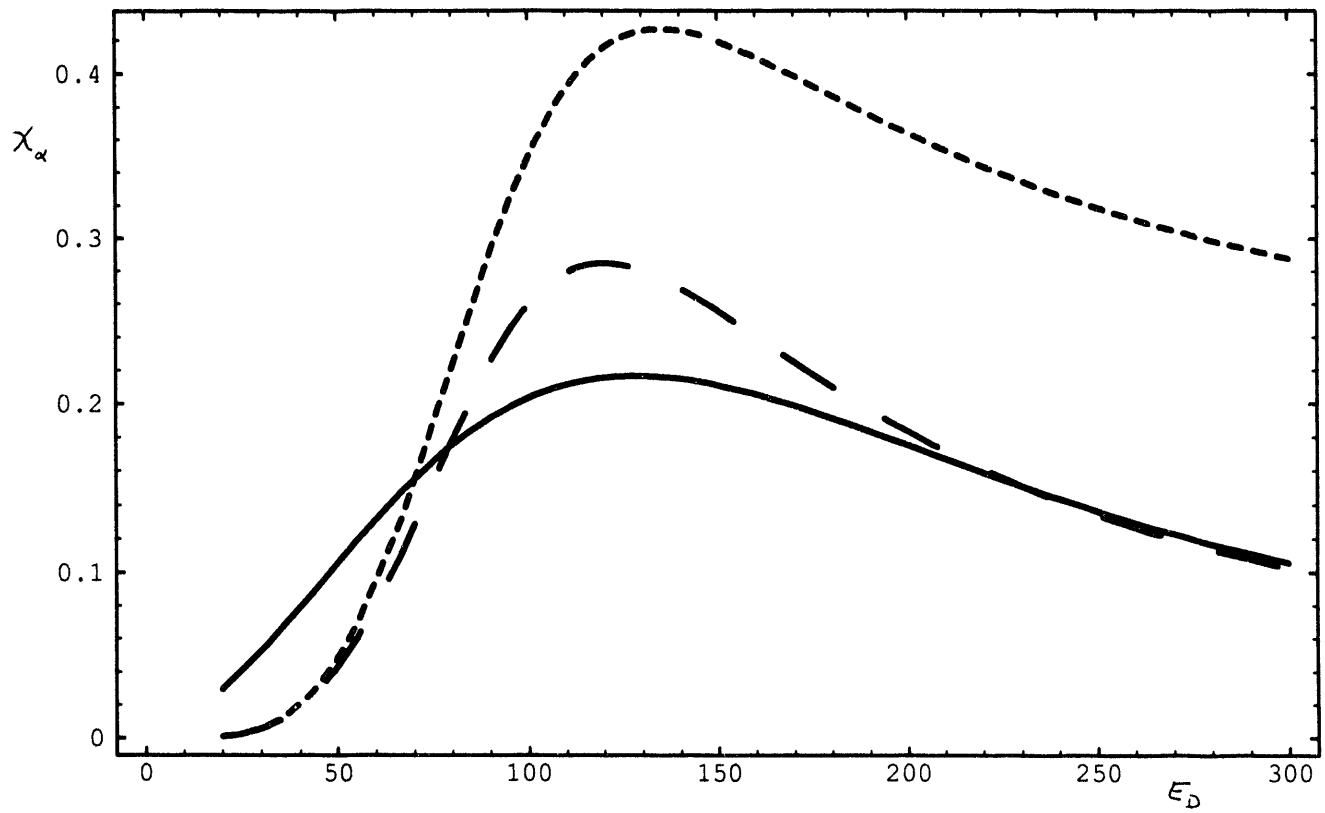

Figure 5: χ_α versus deuterium ion energy for a 50:50 D-T mixture, for $T_e \rightarrow \infty$, T_T=0 KeV (dotted line); for T_e=10 KeV, T_T=0 KeV (dashed line); and for T_e=10 KeV, T_T=20 KeV (solid line).

EXTERNAL DISTRIBUTION IN ADDITION TO UC-420

Dr. F. Paoloni, Univ. of Wollongong, AUSTRALIA
Prof. M.H. Brennan, Univ. of Sydney, AUSTRALIA
Plasma Research Lab., Australian Nat. Univ., AUSTRALIA
Prof. I.R. Jones, Flinders Univ, AUSTRALIA
Prof. F. Cap, Inst. for Theoretical Physics, AUSTRIA
Prof. M. Heindler, Institut für Theoretische Physik, AUSTRIA
Prof. M. Goossens, Astronomisch Instituut, BELGIUM
Ecole Royale Militaire, Lab. de Phy. Plasmas, BELGIUM
Commission-European, DG. XII-Fusion Prog., BELGIUM
Prof. R. Boucique, Rijksuniversiteit Gent, BELGIUM
Dr. P.H. Sakanaka, Instituto Fisica, BRAZIL
Prof. Dr. I.C. Nascimento, Instituto Fisica, Sao Paulo, BRAZIL
Instituto Nacional De Pesquisas Espaciais-INPE, BRAZIL
Documents Office, Atomic Energy of Canada Ltd., CANADA
Ms. M. Morin, CCFM/Tokamak de Varennes, CANADA
Dr. M.P. Bachynski, MPB Technologies, Inc., CANADA
Dr. H.M. Skarsgard, Univ. of Saskatchewan, CANADA
Prof. J. Teichmann, Univ. of Montreal, CANADA
Prof. S.R. Sreenivasan, Univ. of Calgary, CANADA
Prof. T.W. Johnston, INRS-Energie, CANADA
Dr. R. Bolton, Centre canadien de fusion magnétique, CANADA
Dr. C.R. James,, Univ. of Alberta, CANADA
Dr. P. Lukác, Komenského Universzita, CZECHO-SLOVAKIA
The Librarian, Culham Laboratory, ENGLAND
Library, R61, Rutherford Appleton Laboratory, ENGLAND
Mrs. S.A. Hutchinson, JET Library, ENGLAND
Dr. S.C. Sharma, Univ. of South Pacific, FIJI ISLANDS
P. Mähönen, Univ. of Helsinki, FINLAND
Prof. M.N. Bussac, Ecole Polytechnique,, FRANCE
C. Mouttet, Lab. de Physique des Milieux Ionisés, FRANCE
J. Radet, CEN/CADARACHE - Bat 506, FRANCE
Prof. E. Economou, Univ. of Crete, GREECE
Ms. C. Rinni, Univ. of Ioannina, GREECE
Preprint Library, Hungarian Academy of Sci., HUNGARY
Dr. B. DasGupta, Saha Inst. of Nuclear Physics, INDIA
Dr. P. Kaw, Inst. for Plasma Research, INDIA
Dr. P. Rosenau, Israel Inst. of Technology, ISRAEL
Librarian, International Center for Theo Physics, ITALY
Miss C. De Palo, Associazione EURATOM-ENEA , ITALY
Dr. G. Grosso, Istituto di Fisica del Plasma, ITALY
Prof. G. Rostangni, Istituto Gas Ionizzati Del Cnr, ITALY
Dr. H. Yamato, Toshiba Res & Devel Center, JAPAN
Prof. I. Kawakami, Hiroshima Univ., JAPAN
Prof. K. Nishikawa, Hiroshima Univ., JAPAN
Librarian, Naka Fusion Research Establishment, JAERI, JAPAN
Director, Japan Atomic Energy Research Inst., JAPAN
Prof. S. Itoh, Kyushu Univ., JAPAN
Research Info. Ctr., National Instit. for Fusion Science, JAPAN
Prof. S. Tanaka, Kyoto Univ., JAPAN
Library, Kyoto Univ., JAPAN
Prof. N. Inoue, Univ. of Tokyo, JAPAN
Secretary, Plasma Section, Electrotechnical Lab., JAPAN
S. Mori, Technical Advisor, JAERI, JAPAN
Dr. O. Mitarai, Kumamoto Inst. of Technology, JAPAN
Dr. G.S. Lee, Korea Basic Sci. Ctr., KOREA
J. Hyeon-Sook, Korea Atomic Energy Research Inst., KOREA
D.I. Choi, The Korea Adv. Inst. of Sci. & Tech., KOREA
Prof. B.S. Liley, Univ. of Waikato, NEW ZEALAND
Inst of Physics, Chinese Acad Sci PEOPLE'S REP. OF CHINA
Library, Inst. of Plasma Physics, PEOPLE'S REP. OF CHINA
Tsinghua Univ. Library, PEOPLE'S REPUBLIC OF CHINA
Z. Li, S.W. Inst Physics, PEOPLE'S REPUBLIC OF CHINA
Prof. J.A.C. Cabral, Instituto Superior Tecnico, PORTUGAL
Prof. M.A. Hellberg, Univ. of Natal, S. AFRICA
Prof. D.E. Kim, Pohang Inst. of Sci. & Tech., SO. KOREA
Prof. C.I.E.M.A.T, Fusion Division Library, SPAIN
Dr. L. Stenflo, Univ. of UMEA, SWEDEN
Library, Royal Inst. of Technology, SWEDEN
Prof. H. Wilhelmson, Chalmers Univ. of Tech., SWEDEN
Centre Phys. Des Plasmas, Ecole Polytech, SWITZERLAND
Bibliotheek, Inst. Voor Plasma-Fysica, THE NETHERLANDS
Asst. Prof. Dr. S. Cakir, Middle East Tech. Univ., TURKEY
Dr. V.A. Glukhikh,Sci. Res. Inst. Electrophys.I Apparatus, USSR
Dr. D.D. Ryutov, Siberian Branch of Academy of Sci., USSR
Dr. G.A. Eliseev, I.V. Kurchatov Inst., USSR
Librarian, The Ukr.SSR Academy of Sciences, USSR
Dr. L.M. Kovrizhnykh, Inst. of General Physics, USSR
Kernforschungsanlage GmbH, Zentralbibliothek, W. GERMANY
Bibliothek, Inst. Für Plasmaforschung, W. GERMANY
Prof. K. Schindler, Ruhr-Universität Bochum, W. GERMANY
Dr. F. Wagner, (ASDEX), Max-Planck-Institut, W. GERMANY
Librarian, Max-Planck-Institut, W. GERMANY

DATE
FILMED
6/16/94
END